

# LITHOS

## Recycled crustal carbon in the depleted mantle source of El Hierro volcano, Canary Islands.

--Manuscript Draft--

<b>Manuscript Number:</b>	
<b>Article Type:</b>	Regular Article
<b>Keywords:</b>	Canary Islands; El Hierro; mantle xenoliths; fluid inclusions; recycled carbon; noble gases
<b>Corresponding Author:</b>	Andres Libardo Sandoval Velasquez Università degli Studi di Palermo: Università degli Studi di Palermo Palermo, Sicily ITALY
<b>First Author:</b>	Andres Sandoval Velasquez
<b>Order of Authors:</b>	Andres Sandoval Velasquez Andrea Luca Rizzo Alessandro Aiuppa Samantha Remigi Eleazar Padrón Nemesio M. Pérez Maria Luce Frezzotti
<b>Abstract:</b>	<p>The Canary Islands, in the eastern Atlantic, is among the most enigmatic Oceanic Island provinces on Earth, as the mantle source feeding its volcanism exhibits wide spatial heterogeneity and multiplicity of sources. Multi-isotope whole-rock studies have long revealed the presence of a recycled oceanic crust/lithosphere component in the mantle source. However, noble gas systematics have been more challenging to interpret, and carbon isotope constraints have to date remained unavailable to support/dismiss this interpretation. Here, we present the very first isotopic characterisation of CO<sub>2</sub> and noble gases (He-Ne-Ar) in fluid inclusions (FI) in minerals hosted in mantle xenoliths from El Hierro, the youngest and westernmost island of the Canary volcanic archipelago. Six fresh xenoliths from El Julan cliff valley were analysed (3 spinel lherzolites and 3 spinel harzburgites). We find carbon isotopic compositions of CO<sub>2</sub> in FI (<math>\delta^{13}\text{C}</math>) ranging from <math>-2.38</math> to <math>-1.23\%</math> in pyroxenes and from <math>-0.19</math> to <math>+0.96\%</math> in olivines. These unusually positive <math>\delta^{13}\text{C}</math> values, well above the typical mantle range (<math>-8\% &lt; \delta^{13}\text{C} &lt; -4\%</math>), prove, for the first time, the presence of a recycled crustal carbon component in the local source mantle. We interpret this <math>^{13}\text{C}</math>-rich component as inherited from a mantle metasomatism event driven by fluids carrying carbon from C. In contrast, our El Hierro xenoliths identify a depleted mantle-like He signature, with an average Rc/Ra ratio (<math>^3\text{He}/^4\text{He}</math> normalised to air ratio and corrected for atmospheric contamination) of <math>7.45 \pm 0.26 \text{ Ra}</math>. The involvement of depleted mantle-like fluids, variably admixed with air-derived components (possibly recycled via paleo-subduction event(s)), is corroborated by Ne-Ar isotopic compositions. The depleted mantle-like He signature points against the involvement of a primordial He source in the local lithospheric mantle and proves a marginal role played by past subduction events in modifying the local mantle He budget. When put in the context of previous <math>^3\text{He}/^4\text{He}</math> measurements in FI and surface gases along the Canary archipelago, our results confirm an overall west-to-east decrease of Rc/Ra ratios, which may be interpreted as due to increasing contributions from the African sub-continental mantle, the addition of radiogenic <math>^4\text{He}</math> during magma migration in the oceanic crust (whose thickness increases eastward) and/or magma ageing.</p>
<b>Suggested Reviewers:</b>	Peter Barry Woods Hole Oceanographic Institution pbarry@whoi.edu  Ray Burgess The University of Manchester

	ray.burgess@manchester.ac.uk
	Theodoros Ntaflos University of Vienna: Universitat Wien theodoros.ntaflos@univie.ac.at
<b>Opposed Reviewers:</b>	

1 **Recycled crustal carbon in the depleted mantle source of El Hierro volcano,**  
2 **Canary Islands.**

3

4 A. Sandoval-Velasquez<sup>1</sup>, A.L. Rizzo<sup>2</sup>, A. Aiuppa<sup>1,2</sup>, S. Remigi<sup>3</sup>, E. Padrón<sup>4,5</sup>, N. M. Pérez<sup>4,5</sup> and M.L. Frezzotti<sup>3</sup>

5 **Author's affiliations**

6 <sup>1</sup>*DiSTeM, Università di Palermo, Via Archirafi 36, 90123 Palermo, Italy.*

7 <sup>2</sup>*Istituto Nazionale di Geofisica e Vulcanologia (INGV), Sezione di Palermo, Via Ugo La Malfa 153, 90146*  
8 *Palermo, Italy,*

9 <sup>3</sup>*Dipartimento di Scienze dell'Ambiente e della Terra, Università di Milano Bicocca, Piazza della Scienza 4,*  
10 *20126 Milano, Italy,*

11 <sup>4</sup>*Instituto Tecnológico y de Energías Renovables, S.A. (ITER, S.A.), Granadilla de Abona, Tenerife, Canary*  
12 *Islands, Spain,*

13 <sup>5</sup>*Instituto Volcanológico de Canarias (INVOLCAN), San Cristóbal de La Laguna, Tenerife, Canary Islands,*  
14 *Spain.*

15 **Corresponding author e-mail:** andreslibardo.sandovalvelasquez@community.unipa.it



# UNIVERSITÀ DEGLI STUDI DI PALERMO

Dipartimento di Scienze della Terra e del Mare (DiSTeM)

COD. FISC. 80023730825 ~ P.IVA 00605880822

**Editor in Chief**  
**Lithos**

Palermo, 29 April 2021

We are pleased to submit the manuscript entitled “Recycled crustal carbon in the depleted mantle source of El Hierro volcano, Canary Islands.” for consideration for publication in *Lithos*. This paper is the result of a collaborative effort between the University of Palermo, the Istituto Nazionale di Geofisica e Vulcanologia (INGV), the University of Milano-Bicocca, the Instituto Tecnológico y de Energías Renovables, S.A. (ITER, S.A.), (Tenerife, Canary Islands, Spain) and the Instituto Volcanológico de Canarias (INVOLCAN) (Tenerife, Canary Islands, Spain).

In this work, we report on the first isotopic results for CO<sub>2</sub> and noble gas in fluid inclusions trapped in mantle xenoliths collected from El Hierro, the youngest oceanic island in the Canary Islands. The CO<sub>2</sub> carbon isotopic compositions, the first-ever reported for El Hierro, prove the existence of a recycled crustal carbon component in the local source mantle. This component reflects the infiltration of metasomatic fluids, that we interpret as resulting from subducted altered oceanic crust (AOC) and/or oceanic lithosphere (OL), consistent with independent geochemical evidence (chemical and isotope tracers). Noble gas compositions in fluid inclusions constrain a MORB-like signature of the mantle beneath El Hierro, integrating the evidence of volcanic gases and erupted rocks. A careful review of <sup>3</sup>He/<sup>4</sup>He data available for the Canary Islands is also undertaken that offers new insights to interpret the west-to-east isotopic variation over the archipelago. We propose that the <sup>3</sup>He/<sup>4</sup>He depletion observed in the eastern islands may reflect a combination of an Enriched Mantle (EM) component in the mantle with magma ageing and/or assimilation of radiogenic He upon its ascent and ponding in the crust. Ultimately, our study provides new and valuable information on carbon and noble gas stored in/cycling through the Earth’s mantle beneath the complex geodynamic setting of Canary magmatism.

We believe that this manuscript will be of interest to a wide range of scientists working in a variety of Earth Science topics, and we hope it can be considered for publication in *Lithos*.

Sincerely,

Corresponding author.

  
**Andrés Libardo Sandoval Velásquez**

## 1 ABSTRACT

2 The Canary Islands, in the eastern Atlantic, is among the most enigmatic Oceanic Island provinces on Earth,  
3 as the mantle source feeding its volcanism exhibits wide spatial heterogeneity and multiplicity of sources.  
4 Multi-isotope whole-rock studies have long revealed the presence of a recycled oceanic crust/lithosphere  
5 component in the mantle source. However, noble gas systematics have been more challenging to interpret, and  
6 carbon isotope constraints have to date remained unavailable to support/dismiss this interpretation. Here, we  
7 present the very first isotopic characterisation of CO<sub>2</sub> and noble gases (He-Ne-Ar) in fluid inclusions (FI) in  
8 minerals hosted in mantle xenoliths from El Hierro, the youngest and westernmost island of the Canary  
9 volcanic archipelago. Six fresh xenoliths from El Julan cliff valley were analysed (3 spinel lherzolites and 3  
10 spinel harzburgites). We find carbon isotopic compositions of CO<sub>2</sub> in FI ( $\delta^{13}\text{C}$ ) ranging from  $-2.38$  to  $-1.23\%$   
11 in pyroxenes and from  $-0.19$  to  $+0.96\%$  in olivines. These unusually positive  $\delta^{13}\text{C}$  values, well above the  
12 typical mantle range ( $-8\% < \delta^{13}\text{C} < -4\%$ ), prove, for the first time, the presence of a recycled crustal carbon  
13 component in the local source mantle. We interpret this  $^{13}\text{C}$ -rich component as inherited from a mantle  
14 metasomatism event driven by fluids carrying carbon from C. In contrast, our El Hierro xenoliths identify a  
15 depleted mantle-like He signature, with an average R<sub>c</sub>/R<sub>a</sub> ratio ( $^3\text{He}/^4\text{He}$  normalised to air ratio and corrected  
16 for atmospheric contamination) of  $7.45 \pm 0.26$  R<sub>a</sub>. The involvement of depleted mantle-like fluids, variably  
17 admixed with air-derived components (possibly recycled via paleo-subduction event(s)), is corroborated by  
18 Ne-Ar isotopic compositions. The depleted mantle-like He signature points against the involvement of a  
19 primordial He source in the local lithospheric mantle and proves a marginal role played by past subduction  
20 events in modifying the local mantle He budget. When put in the context of previous  $^3\text{He}/^4\text{He}$  measurements  
21 in FI and surface gases along the Canary archipelago, our results confirm an overall west-to-east decrease of  
22 R<sub>c</sub>/R<sub>a</sub> ratios, which may be interpreted as due to increasing contributions from the African sub-continental  
23 mantle, the addition of radiogenic  $^4\text{He}$  during magma migration in the oceanic crust (whose thickness increases  
24 eastward) and/or magma ageing.

1 **Recycled crustal carbon in the depleted mantle source of El Hierro volcano,**  
2 **Canary Islands.**

3

4 A. Sandoval-Velasquez<sup>1</sup>, A.L. Rizzo<sup>2</sup>, A. Aiuppa<sup>1,2</sup>, S. Remigi<sup>3</sup>, E. Padrón<sup>4,5</sup>, N. M. Pérez<sup>4,5</sup> and M.L. Frezzotti<sup>3</sup>

5

6 **Highlights**

- 7
- $\delta^{13}\text{C}$  of  $\text{CO}_2$  in fluid inclusions tracks recycled crustal carbon in the El Hierro mantle source
- 8
- Crustal carbon may derive from subducted altered oceanic crust or lithosphere
- 9
- Noble gases indicate the MORB-like signature of the mantle beneath El Hierro
- 10
- Increasing crustal contribution concurs to the west-to-east  $^3\text{He}/^4\text{He}$  decrease in the Canary

[Click here to view linked References](#)

1 **Recycled crustal carbon in the depleted mantle source of El Hierro volcano,**  
2 **Canary Islands.**

3

4 A. Sandoval-Velasquez<sup>1</sup>, A.L. Rizzo<sup>2</sup>, A. Aiuppa<sup>1,2</sup>, S. Remigi<sup>3</sup>, E. Padrón<sup>4,5</sup>, N. M. Pérez<sup>4,5</sup> and M.L. Frezzotti<sup>3</sup>

5 **Author's affiliations**

6 <sup>1</sup>*DiSTeM, Università di Palermo, Via Archirafi 36, 90123 Palermo, Italy.*

7 <sup>2</sup>*Istituto Nazionale di Geofisica e Vulcanologia (INGV), Sezione di Palermo, Via Ugo La Malfa 153, 90146*  
8 *Palermo, Italy,*

9 <sup>3</sup>*Dipartimento di Scienze dell'Ambiente e della Terra, Università di Milano Bicocca, Piazza della Scienza 4,*  
10 *20126 Milano, Italy,*

11 <sup>4</sup>*Instituto Tecnológico y de Energías Renovables, S.A. (ITER, S.A.), Granadilla de Abona, Tenerife, Canary*  
12 *Islands, Spain,*

13 <sup>5</sup>*Instituto Volcanológico de Canarias (INVOLCAN), San Cristóbal de La Laguna, Tenerife, Canary Islands,*  
14 *Spain.*

15 **Corresponding author e-mail:** andreslibardo.sandovalvelasquez@community.unipa.it

16 **ABSTRACT**

17 The Canary Islands, in the eastern Atlantic, is among the most enigmatic Oceanic Island provinces on Earth,  
18 as the mantle source feeding its volcanism exhibits wide spatial heterogeneity and multiplicity of sources.

19 Multi-isotope whole-rock studies have long revealed the presence of a recycled oceanic crust/lithosphere  
20 component in the mantle source. However, noble gas systematics have been more challenging to interpret, and  
21 carbon isotope constraints have to date remained unavailable to support/dismiss this interpretation. Here, we  
22 present the very first isotopic characterisation of CO<sub>2</sub> and noble gases (He-Ne-Ar) in fluid inclusions (FI) in  
23 minerals hosted in mantle xenoliths from El Hierro, the youngest and westernmost island of the Canary  
24 volcanic archipelago. Six fresh xenoliths from El Julan cliff valley were analysed (3 spinel lherzolites and 3  
25 spinel harzburgites). We find carbon isotopic compositions of CO<sub>2</sub> in FI ( $\delta^{13}\text{C}$ ) ranging from  $-2.38$  to  $-1.23\%$

26 in pyroxenes and from  $-0.19$  to  $+0.96\text{‰}$  in olivines. These unusually positive  $\delta^{13}\text{C}$  values, well above the  
27 typical mantle range ( $-8\text{‰} < \delta^{13}\text{C} < -4\text{‰}$ ), prove, for the first time, the presence of a recycled crustal carbon  
28 component in the local source mantle. We interpret this  $^{13}\text{C}$ -rich component as inherited from a mantle  
29 metasomatism event driven by fluids carrying carbon from C. In contrast, our El Hierro xenoliths identify a  
30 depleted mantle-like He signature, with an average R<sub>c</sub>/R<sub>a</sub> ratio ( $^3\text{He}/^4\text{He}$  normalised to air ratio and corrected  
31 for atmospheric contamination) of  $7.45 \pm 0.26$  R<sub>a</sub>. The involvement of depleted mantle-like fluids, variably  
32 admixed with air-derived components (possibly recycled via paleo-subduction event(s)), is corroborated by  
33 Ne-Ar isotopic compositions. The depleted mantle-like He signature points against the involvement of a  
34 primordial He source in the local lithospheric mantle and proves a marginal role played by past subduction  
35 events in modifying the local mantle He budget. When put in the context of previous  $^3\text{He}/^4\text{He}$  measurements  
36 in FI and surface gases along the Canary archipelago, our results confirm an overall west-to-east decrease of  
37 R<sub>c</sub>/R<sub>a</sub> ratios, which may be interpreted as due to increasing contributions from the African sub-continental  
38 mantle, the addition of radiogenic  $^4\text{He}$  during magma migration in the oceanic crust (whose thickness increases  
39 eastward) and/or magma ageing.

40 **Keywords:** *Canary Islands, El Hierro, mantle xenoliths, fluid inclusions, recycled carbon, noble gases.*

41

## 42 **1. INTRODUCTION**

43 In Ocean Island and intra-plate settings, mantle heterogeneities have often been invoked to justify the  
44 variability of geochemical tracers (e.g., He, Sr, Nd, and Pb isotopes; Hofmann, 1997, 2003; Jackson and  
45 Dasgupta, 2008; Dasgupta et al., 2010; Day et al., 2010; Day and Hilton, 2011, 2020). These heterogeneities  
46 would derive from the long-term preservation of depleted and enriched components variably and locally  
47 mixing into the mantle (see Hofmann, 1997, 2003 for a review). Some of these components relate to recycling  
48 old subducted materials that lead to extreme isotopic signatures (e.g., Sobolev et al., 2007).

49 The study of the isotopic composition of fluids trapped in mantle xenoliths (e.g., Deines, 2002; Gautheron and  
50 Moreira, 2002; Pearson et al., 2014; Day et al., 2015) may help better-comprehending mantle features and  
51 evolution back in time, as they provide clues on the origin and cycling of volatiles in the Earth's interior. Noble  
52 gases in mantle xenoliths, in particular, are proven tools for constraining the relative mixing proportions among



53 different mantle reservoirs (e.g., Gurenko et al., 2006; Day and Hilton, 2011, 2020; Broadley et al., 2016;  
54 Rizzo et al., 2018; Kobayashi et al., 2019). In addition, carbon isotopes are key species for understanding the  
55 carbon recycling in the lithospheric and deeper mantle via subduction of crustal carbon components (e.g.,  
56 organic matter and sedimentary carbonate) (Dasgupta and Hirschmann, 2010; Aiuppa et al., 2017; Duncan and  
57 Dasgupta, 2017; Li et al., 2019; Plank and Manning, 2019; Regier et al., 2020). Unfortunately, however, carbon  
58 isotope studies in mantle xenoliths are still limited to a relatively small number of localities (Deines, 2002;  
59 Demény et al., 2010; Correale et al., 2015; Gennaro et al., 2017; Boudoire et al., 2018; Rizzo et al., 2018).

60 The Canary Islands represent an ideal laboratory for studying heterogeneities in noble gas and carbon mantle  
61 signatures, as ultramafic xenoliths, volcanic rocks, and surface emissions associated with the active volcanism  
62 of the archipelago prove the involvement of multiple sources at play the mantle source (Gurenko et al., 2006;  
63 Day and Hilton, 2020). The origin of volcanism in the Canary Islands is still a matter of debate, given the area's  
64 geodynamic and tectonic complexity (Anguita and Hernán, 2000). There is consensus, however, that a mantle  
65 plume model fits most of the geophysical and geochemical evidence (Fig. 1; Hoernle and Schmincke, 1993;  
66 Pérez et al., 1994; Hoernle et al., 1995; Carracedo et al., 1998; Montelli, 2004; Day et al., 2010; Day and  
67 Hilton, 2020). However, in terms of noble gases, only the geothermal gases of the Taburiente caldera (La  
68 Palma island), with their  $^3\text{He}/^4\text{He}$  of  $> 9\text{Ra}$  (where Ra is the  $^3\text{He}/^4\text{He}$  atmospheric ratio), identify a primordial  
69 component in the Canary mantle source (Pérez et al., 1994, 1996; Hilton et al., 2000; Day and Hilton, 2020;  
70 Fig. 1). In contrast, volcanic rocks of the same island record a depleted mantle (MORB; Middle Oceanic Ridge  
71 Basalt) signature (e.g., Hilton et al., 2000), and other Islands ( $^3\text{He}/^4\text{He}$  are available for El Hierro, Gran Canaria,  
72 Tenerife, La Gomera, Fuerteventura and Lanzarote) generally exhibit MORB-like, or even more radiogenic  
73 (lower  $^3\text{He}/^4\text{He}$  ratios) signatures (see Fig.1 and Table S1 for isotopic values and references). These variations  
74 have been taken as evidence of mantle heterogeneities in the sources of magmas. In particular, steaming from  
75 multi-isotope (He-Nd-Sr-Pb-Os-O) results, an Enriched Mantle (EM) component has been proposed in the  
76 eastern portion of the archipelago (Hoernle et al., 1991; Carnevale et al., 2021), while a HIMU (High- $\mu$ =  
77 elevated  $^{238}\text{U}/^{204}\text{Pb}$ ) mantle signature has been identified in its western edge (Gurenko et al., 2006; Day and  
78 Hilton, 2011, 2020). These results prove that recycled volatiles (e.g., derived from melting of old subducted  
79 oceanic crust/lithosphere in the case of the HIMU component) get admixed with depleted (MORB) and plume  
80 mantle sources underneath the archipelago (Day and Hilton, 2011, 2020).

81 One complication in these interpretations is that most  $^3\text{He}/^4\text{He}$  measurements refer to volcanic gases and/or FI  
82 in lava phenocrysts (measured with different extraction techniques) that can be affected by secondary and  
83 shallow processes. For example, FI may be susceptible to the addition of cosmogenic  $^3\text{He}$  and/or radiogenic  
84  $^4\text{He}$ , and to diffusive He loss from crystals, while volcanic gases can suffer from shallow contamination by  
85 crustal and atmospheric fluids. Therefore, noble gas results on mantle xenoliths are urgently needed to  
86 constrain the mantle signature beneath each island in the Canary archipelago.

87 The case is exacerbated even more for carbon, whose origin has mainly been inferred from the isotopic  
88 composition of  $\text{CO}_2$  ( $\delta^{13}\text{C}$ ) in volcanic gases and groundwaters from La Palma and Tenerife, and generically  
89 considered of magmatic or mantle origin (see supplementary Table S1 for isotopic values and references).  
90 Thus, whether or not a recycled carbon component exists in the Canary source mantle remains unanswered.  
91 As subduction of altered ocean crust/lithosphere is a crucial pathway for the return of shallow crustal carbon  
92 back into the mantle (Alt and Teagle, 1999; Alt et al., 2013; Hazen et al., 2013; Hammouda and Keshav, 2015;  
93 Martin and Hermann, 2018; Plank and Manning, 2019), the existence of recycled carbon underneath western  
94 Canary is expected (but yet unproven) given the HIMU affinity of the erupted magmas.

95 Here, we present the first isotopic measurements of noble gases and  $\text{CO}_2$  in fluid inclusions (FI) in mantle  
96 xenoliths from El Hierro, the youngest oceanic island of the Canary (Carracedo et al., 1998) and where  
97 occurred the most recent eruption in 2011-2012 (Padrón et al., 2013). From this, we constrain the  $^3\text{He}/^4\text{He}$   
98 signature of the mantle beneath El Hierro that, combined with a careful review of existing data, offer new  
99 insights to interpret the west-to-east He variability along the archipelago. Our  $\text{CO}_2$  isotope compositions, the  
100 first-ever reported for El Hierro, and the first FI results for the Canary archipelago, allow us recognising a  
101 recycled crustal carbon component in the local source mantle.

102

## 103 **2. GEOLOGICAL AND VOLCANOLOGICAL SETTING**

104 The Canary Islands are an archipelago composed of 7 main volcanic islands (from East to West: Lanzarote,  
105 Fuerteventura, Gran Canaria, Tenerife, La Gomera, La Palma and El Hierro) located in front of the western  
106 coast of North Africa and extended for almost 500 km (Fig. 1). The volcanic islands and seamounts formed on  
107 oceanic lithosphere of Jurassic age close to a passive continental margin (Schmincke, 1982; Carracedo et al.,

108 1998; Anguita and Hernán, 2000; Troll and Carracedo, 2016). Although the volcanism that formed the Canary  
109 started more than 20 Ma, ages between 47 and 142 Ma have been also reported for the old seamounts located  
110 NE and SW of the archipelago (Schmincke, 1982; Carracedo et al., 1998; van den Bogaard, 2013). Quaternary  
111 volcanic deposits have been reported along the Canary Islands (except for La Gomera) and most of them are  
112 considered volcanically active (Carracedo et al., 1998; Troll and Carracedo, 2016). The most recent eruption  
113 was registered in 2011-2012 in El Hierro (Padrón et al., 2013).

114 The Canary Islands exhibit an enormous spectrum of volcanic rocks, from carbonatites, nephelinites, basanites,  
115 tephrites, tholeiitic and alkali olivine basalts associated with shield-volcanism processes to rhyodacites,  
116 rhyolites, trachytes and phonolites related to a highly explosive felsic volcanism (Schmincke, 1982; Abratis et  
117 al., 2002; Carracedo et al., 1998; Troll and Carracedo, 2016). It is worth mentioning that this magmatic activity  
118 has brought to the surface important quantities of ultramafic xenoliths along the entire archipelago (e.g.,  
119 Admunsen, 1987; Siena et al., 1991; Neumann and Wulff-Pedersen, 1997; Frezzotti et al., 2002b; Oglialoro et  
120 al., 2017).

121 Several hypotheses have been formulated about the origin of the Canary Islands: Anguita and Hernan (1975)  
122 proposed a connection between the Islands and the Atlas Mountains by a mega-shear that experienced a  
123 tensional phase causing decompression melting and volcanism. Araña and Ortiz (1991) suggested that  
124 compressive tectonics are the cause of the magmatism and the uplift of the archipelago; instead, Hoernle and  
125 Schmincke (1993) and Carracedo et al. (1998) described a mantle plume model where volcanism is generated  
126 by a thermal mantle anomaly (a hot-spot) which is supported by geochemical evidence, the progressive west-  
127 to-east age increase of the islands and the relative movement of the African plate (approximately 2 cm/year;  
128 Carracedo et al., 1998). Finally, Anguita and Hernán (2000) integrated these hypotheses and proposed a unified  
129 model to explain the complexity of the thermal and tectonic evolution of the Canary Islands.

130 El Hierro is the youngest (1.12 Ma) and westernmost island of the Canary and its history is summarized in  
131 three stages (Troll and Carracedo, 2016 and references therein): (i) the formation of the Triño Volcano (1.12  
132 Ma to 1.03 Ma); (ii) the collapse of the latter and the emplacement of a new volcanic structure (the Golfo  
133 volcano; 545 – 176 ka), and (iii) the development of a triple rift system where most of the recent volcanism  
134 has focused. This volcanism is mainly dominated by high alkali silica-saturated rocks and Hawaiian-type

135 tholeiites (extruded during the Golfo volcano eruption), which may contain ultramafic xenoliths (Neumann,  
136 1991; Oglialoro et al., 2017).

137

### 138 3. SAMPLES AND METHODS

139 The analysed suite of mantle xenoliths consists of 3 spinel lherzolites and 3 spinel harzburgites selected among  
140 over 35 peridotite samples from El Julan cliff valley, El Hierro (Canary Islands; Fig. 1), and erupted 30 – 40  
141 ka ago (Oglialoro et al., 2017). Sampling details and petrographic characteristics of these rocks are already  
142 presented elsewhere (Oglialoro et al., 2017; Colombo, 2020). For the present study, sample selection was  
143 performed based on the type of fluid and melt inclusions present to sample metasomatic CO<sub>2</sub>-rich fluids in the  
144 lithospheric mantle (Frezzotti et al., 2012b; Frezzotti and Touret, 2014), limiting the contribution of CO<sub>2</sub> in FI  
145 formed during degassing of host basanitic magmas during ascent. In selected peridotites, FI coexist with a  
146 complex network of glass microveins. Two types of FI are present: CO<sub>2</sub> (±N<sub>2</sub>) and CO<sub>2</sub> (±N<sub>2</sub> traces) + daughter  
147 minerals (>70% in volume), including anhydrite, Mg-calcite, dolomite, hydrated Mg-sulphate; sulphohalite;  
148 apatite; spinel; magnesite, and talc (Oglialoro et al., 2017; Remigi et al., 2019). Microveins contain silicate  
149 glass and carbonate droplets and are present in olivine (Ol) grains, and along Ol and orthopyroxene (Opx)  
150 grain boundaries. Maximum calculated densities of CO<sub>2</sub>-N<sub>2</sub> are extremely high, up to 1.19 g/cm<sup>3</sup>,  
151 corresponding to fluid trapping at 1.8±0.02 GPa or about 65 km depth (at 950°C; Oglialoro et al., 2017).

152 For noble gas and CO<sub>2</sub> analysis, xenoliths were crushed and sieved to handpick fresh and unaltered crystals of  
153 Ol, Opx, and Cpx with diameters generally ≥0.5 mm. The noble gas and CO<sub>2</sub> concentrations and isotopic ratios  
154 of FI were investigated at the noble gas and stable isotopes laboratories of INGV, Sezione di Palermo (Italy),  
155 following the preparation and analytical techniques described in Gennaro et al. (2017) and Rizzo et al. (2018).  
156 Before noble gas determinations, samples were cleaned in an ultrasonic bath in 6.5% HNO<sub>3</sub>, in deionised water  
157 and high-purity acetone. After then, samples were weighed and loaded into an ultra-high-vacuum crusher for  
158 noble gas analyses, where the first estimate of the concentration of CO<sub>2</sub> in FI was performed. The estimation  
159 of CO<sub>2</sub> was performed by measuring the total pressure of gas (CO<sub>2</sub>+N<sub>2</sub>+O<sub>2</sub>+noble gases) released during  
160 crushing (by an IONIVAC Transmitters ITR90) in a known volume of the system, then the residual pressure  
161 of N<sub>2</sub>+O<sub>2</sub>+noble gases was subtracted after removing CO<sub>2</sub> in a “cold finger” immersed in liquid nitrogen. FI

162 were released by single-step crushing at about 200 bar and room temperature (21°C) to prevent/limit the  
 163 addition of cosmogenic and radiogenic helium accumulated in the crystal lattices (Kurz, 1986; Graham, 2002;  
 164 Rizzo et al., 2018; Correale et al., 2019). After the manometric determination of the CO<sub>2</sub> concentration, the  
 165 resulting gas mixture was purified in a stainless-steel ultra-high-vacuum preparation line to remove all gas  
 166 species (N<sub>2</sub>, H<sub>2</sub>, H<sub>2</sub>O, CO<sub>2</sub>) except noble gases. Then, Ar was adsorbed in a charcoal trap submerged in liquid  
 167 nitrogen. He and Ne were finally adsorbed in a cryogenic trap in which a charcoal trap is in contact with a cold  
 168 head cooled down at about 10 °K by a helium compressor, and separately released at about 42 and 83 °K,  
 169 respectively. Once desorbed, He and Ne were admitted in two distinct split-flight-tube mass spectrometers  
 170 (Helix SFT, Thermo Scientific), while Ar in a multi-collector mass spectrometer (Argus, GVI). Analytical  
 171 uncertainties (2σ) for <sup>3</sup>He/<sup>4</sup>He, <sup>20</sup>Ne/<sup>22</sup>Ne, <sup>21</sup>Ne/<sup>22</sup>Ne, <sup>40</sup>Ar/<sup>36</sup>Ar, and <sup>38</sup>Ar/<sup>36</sup>Ar ratios are <0.94%, <0.07%,  
 172 <0.328%, <0.0614%, and <0.0945%, respectively. Further details on the type and analytical uncertainty of  
 173 adopted standards and their reproducibility over time and blank levels can be found in Rizzo et al. (2018) that  
 174 followed analogous protocols.

175 Abundances of He (<sup>3</sup>He, <sup>4</sup>He), Ne (<sup>20</sup>Ne, <sup>21</sup>Ne, <sup>22</sup>Ne) and Ar (<sup>36</sup>Ar, <sup>40</sup>Ar and <sup>40</sup>Ar\*) isotopes are determined.  
 176 <sup>3</sup>He/<sup>4</sup>He ratios are reported as R/Ra (where R is the <sup>3</sup>He/<sup>4</sup>He ratio of the sample and Ra the <sup>3</sup>He/<sup>4</sup>He ratio of air  
 177 = 1.384×10<sup>-6</sup>; Clarke et al., 1976). Although most of the samples showed low atmospheric contamination (air  
 178 has <sup>4</sup>He/<sup>20</sup>Ne = 0.318, <sup>20</sup>Ne/<sup>22</sup>Ne = 9.8, <sup>21</sup>Ne/<sup>22</sup>Ne = 0.029, and <sup>40</sup>Ar/<sup>36</sup>Ar = 295.5; Ozima and Podosek, 2001),  
 179 <sup>3</sup>He/<sup>4</sup>He was corrected for contamination based on the measured <sup>4</sup>He/<sup>20</sup>Ne ratio as follows:

$$180 \quad R_c/R_a = ((R_M/R_a)(\text{He/Ne})_M - (\text{He/Ne})_A)/((\text{He/Ne})_M - (\text{He/Ne})_A) \quad \text{eq. 1}$$

181  
 182 where subscripts M and A refer to measured and atmospheric theoretical values, respectively. The corrected  
 183 <sup>3</sup>He/<sup>4</sup>He ratios are reported as R<sub>c</sub>/R<sub>a</sub> values. However, the correction was either small or negligible for most  
 184 of the samples.

185 <sup>40</sup>Ar was corrected for air contamination (<sup>40</sup>Ar\*) assuming that the measured <sup>36</sup>Ar was entirely of atmospheric  
 186 origin as follows:

$$187 \quad 188 \quad {}^{40}\text{Ar}^* = {}^{40}\text{Ar}_{\text{sample}} - [{}^{36}\text{Ar}_{\text{sample}} \times ({}^{40}\text{Ar}/{}^{36}\text{Ar})_{\text{air}}] \quad \text{eq. 2}$$

189

$${}^{40}\text{Ar}_{\text{air}} = {}^{40}\text{Ar}_{\text{sample}} - {}^{40}\text{Ar}$$

eq. 3

190

191 After noble gas analysis, seven aliquots with the highest concentrations of CO<sub>2</sub> (2 aliquots of Ol, 4 of Opx and  
192 1 of Cpx) were selected to determine the carbon isotopic composition of FI (<sup>13</sup>C/<sup>12</sup>C) in the stable isotopes  
193 laboratory of INGV-Palermo. Selected crystals were cleaned in an ultrasonic bath in 10% HCl, weighed and  
194 loaded in a crusher system consisting of a stainless- steel sample holder, a hydraulic press (which exerts a  
195 single-step pressure of approximately 200 bar), a glass sampler to freeze CO<sub>2</sub>, and a pump to ensure the vacuum  
196 (10<sup>-3</sup> - 10<sup>-4</sup> mbar) inside the system. During crystals crushing, a glass sampler submerged in liquid nitrogen  
197 was maintained online to freeze CO<sub>2</sub>, and eventually, those gaseous species condensing at a temperature ≥  
198 196°C. Subsequently, the sampler was connected to a glass line equipped with a 626B Baratron® Absolute  
199 Capacitance Manometer MKS (measuring range 10<sup>-3</sup>-10 mbar), for the purification procedure and  
200 quantification of CO<sub>2</sub> concentration (mol/g). The purified CO<sub>2</sub> was condensed in the same glass sampler  
201 (adjusted to atmospheric pressure by adding pure helium) and transferred to the laboratory of stable isotopes  
202 for the following isotopic measurements. The measured <sup>13</sup>C/<sup>12</sup>C ratios are expressed in parts per mil (‰;  
203 relative to the V-PDB international standard) using the delta notation (δ<sup>13</sup>C). The analytical error estimated as  
204 2σ was better than 0.6‰. Further details on the adopted analytical procedure can be found in Gennaro et al.  
205 (2017) and Rizzo et al. (2018) that followed analogous protocols.

206

#### 207 4. RESULTS

208 The elemental and isotopic compositions of noble gases and CO<sub>2</sub> in El Hierro mantle xenoliths are reported in  
209 Table 1. FI composition is dominated by CO<sub>2</sub>, as found previously (Oglialoro et al., 2017). CO<sub>2</sub> exhibits a  
210 broad positive correlation with noble gas and nitrogen concentrations (Fig. S1). Both CO<sub>2</sub> estimates, during  
211 noble gases analysis and CO<sub>2</sub> isotopic determinations (see Table 1), are similar and vary from 5.31x10<sup>-10</sup> to  
212 2.17x10<sup>-6</sup> mol/g. The highest CO<sub>2</sub> concentrations are observed in Cpx (from 7.70x10<sup>-8</sup> to 2.17x10<sup>-6</sup> mol/g),  
213 followed by Opx (from 1.65x10<sup>-8</sup> mol/g to 6.92x10<sup>-7</sup> mol/g) and Ol (from 5.31x10<sup>-10</sup> mol/g to 8.45x10<sup>-8</sup> mol/g).  
214 <sup>4</sup>He/<sup>20</sup>Ne ratios vary between 5.9 and 776.1, with the lowest values measured in sample 1.1 (Opx and Cpx) and  
215 sample 1.23 Cpx. These samples also have low Rc/Ra (<6) and <sup>4</sup>He/<sup>40</sup>Ar\* (<0.07) values, indicating isotopic

216 fractionation during diffusive He loss from FI (see SM1 for details). These samples are thus disregarded in the  
217 further discussion below. The remaining sample aliquots exhibit Rc/Ra values in the 7 to 8 Ra range within  
218 the MORB range (Graham, 2002). The  $^{40}\text{Ar}/^{36}\text{Ar}$ ,  $^{20}\text{Ne}/^{22}\text{Ne}$  and  $^{21}\text{Ne}/^{22}\text{Ne}$  ratios values range from 805.0 to  
219 5328.4, from 9.84 to 10.49, and from 0.0286 to 0.0330, respectively. The spread of Ar and Ne isotopic  
220 signatures is well reproduced by mixing between a depleted mantle (MORB) source and an atmospheric  
221 component (see SM2 for details). The isotopic composition of  $\text{CO}_2$  (expressed as  $\delta^{13}\text{C} = R_{\text{Sample}}/R_{\text{Standard}} - 1$ ,  
222 where  $R = ^{13}\text{C}/^{12}\text{C}$  and the standard is the Vienna Pee Dee Belemnite, VPDB) reveals the highest  $\delta^{13}\text{C}$  values  
223 in Ol (-0.19‰ and +0.96‰), while Opx and Cpx exhibit somewhat more negative compositions, ranging from  
224 -2.38‰ to -1.23‰. These C isotope compositions are well above the typical depleted mantle (MORB) range  
225 (Sano and Marty, 1995).

226

## 227 **5. DISCUSSION**

### 228 *5.1. A depleted mantle noble gas signature for the El Hierro mantle source beneath and the Canary* 229 *archipelago*

230 The average (mean±std deviation) Rc/Ra measured in El Hierro mantle xenoliths is  $7.45\pm 0.26$  Ra (Fig. 2).  
231 This value is comparable to the  $^3\text{He}/^4\text{He}$  values reported in lava phenocrysts and cumulates from the same  
232 island ( $7.66\pm 0.35$  Ra; Fig. 2A), and slightly below the maximum Rc/Ra value measured in groundwater  
233 samples during the 2011-2012 volcanic unrest ( $\sim 8.2$  Ra; Padrón et al., 2013). Averaging these results, we infer  
234 the mean  $^3\text{He}/^4\text{He}$  signature for El Hierro at  $7.58\pm 0.34$  Ra, which we consider representative of the source  
235 mantle. This signature is classically MORB-like, confirming previous indications of a dominant Depleted  
236 MORB Mantle (DMM) source (Day and Hilton, 2011, 2020). Therefore, as additionally implied by Ne and Ar  
237 isotopes (Fig. S2), we find no evidence of primordial noble gas contribution from the lower mantle, as found  
238 instead in the high (Rc/Ra >9) volcanic gases from La Palma (see Table S1). As discussed in Day and Hilton  
239 (2011), the MORB-like Rc/Ra values are evidence for the El Hierro source mantle having been scarcely  
240 impacted by any crustal He addition during past (ancient, 1-2 Ga) oceanic crust/lithosphere subduction events  
241 (implied by the HIMU magma affinity; Hofmann, 1997). It is well possible, instead, that Ne and Ar (being  
242 well more abundant in air and air-saturated seawater than He) are better records of paleo-subduction(s) events,

243 considering that the MORB-air mixing arrays (see SM2 and Fig. S2) may well reflect recycling of atmospheric  
244 gases in the slab. The stable  $^3\text{He}/^4\text{He}$  ratios at El Hierro (Fig. 3B) point to a temporally invariant mantle source  
245 during the last million years (i.e., since the early Pleistocene).

246

## 247 ***5.2. Implications for isotopic variations along the Canary archipelago***

248 We put our El Hierro results in a more general context by comparing them with a suitably revised catalogue  
249 of  $^3\text{He}/^4\text{He}$  ratios measured along the Canary Islands (fumaroles, groundwater, bubbling gas and FI information  
250 from lavas, cumulates, carbonatites, and mantle xenoliths; Table S1, Figs. 2B, 3 and S3). This revised dataset  
251 is built together after filtering out samples affected by secondary processes (diffusive fractionation,  
252 cosmogenic and radiogenic ingrowth of helium) and whose pristine isotopic signature may thus have been  
253 compromised (see SM1 for details). Statistical treatment of the data (Fig. 3A) allows further refinement of this  
254 data filtering, based on the criteria described in SM3. The resulting (after data filtering) isotopic information  
255 is reported in Table S2 and Figs. 3B-3C and 4A-4B.

256 This comparison confirms (Day and Hilton, 2020 and references therein) the presence of a clear lower mantle  
257 component only in volcanic gases from La Palma ( $9.52 \pm 0.32 \text{ Ra}$ ), whereas FI in phenocrysts from the same  
258 island show ratios ( $7.52 \pm 0.66 \text{ Ra}$ ) comparable to those from El Hierro and La Gomera (Fig. 3C). The different  
259  $^3\text{He}/^4\text{He}$  signatures of La Palma and El Hierro have been proposed to derive from mantle sources containing  
260 different proportions of (i) recycled oceanic crust and gabbroic lithosphere (ii) a deep mantle source with  
261  $^3\text{He}/^4\text{He} > 9.7 \text{ Ra}$  (for La Palma) and (iii) the DMM (dominant at El Hierro) (Day and Hilton, 2011, 2020). This  
262 interpretation is reasonably valid also for La Gomera that shows geochemical features similar to the  
263 westernmost islands. Further to the east, from Tenerife to Lanzarote, the  $^3\text{He}/^4\text{He}$  ratios decrease at the lower  
264 end of the MORB range or even below (Fuerteventura and Lanzarote).

265 Based on Sr-Nd-Pb-Os isotopic systematics, the lower  $^3\text{He}/^4\text{He}$  values in Tenerife and eastern Canary have  
266 been suggested to derive from increasing contributions from an enriched mantle (EM) derived from the  
267 incorporation of the continental lithospheric mantle from the West African margin (Hoernle et al., 1991;  
268 Simonsen et al., 2000; Gurenko et al., 2006); Sr-Nd-Pb isotopes in carbonatites from Fuerteventura also  
269 support the existence of such enriched mantle component (Carnevale et al., 2021). While not ruling out this



270 possibility, we also consider the possible role of ascending magma interactions with the oceanic crust, whose  
271 thickness progressively increases eastward (Fig. 3C). As evident in Fig. 3C, the progressive eastward decrease  
272 of the Rc/Ra values that starts in Tenerife (in both volcanic gases and FI) is paralleled by a corresponding  
273 marked increase in crustal thickness (Martinez-Arevalo et al., 2013). Based on this evidence, we argue that the  
274  $^3\text{He}/^4\text{He}$  signature presently observed in samples from Tenerife, Gran Canaria, Fuerteventura, and Lanzarote  
275 may also be controlled by the addition of crustal He during magma-crust interactions. This inference is  
276 plausible if we consider that ascending melts are more prone to be contaminated by the assimilation of crustal-  
277 derived radiogenic  $^4\text{He}$ , lowering the original  $^3\text{He}/^4\text{He}$  values. Accordingly, the high  $^3\text{He}/^4\text{He}$  values observed  
278 mostly in El Hierro and La Palma, but also in La Gomera, would reflect a minimal contribution of crustal  
279 materials. Sr-Nd-Pb-O isotopic ratios indicate crustal assimilation is negligible in lavas erupted from El Hierro  
280 and La Palma (Gurenko et al., 2006; Day et al., 2010). Instead, volcanic rocks from Gran Canaria and  
281 carbonatites from Fuerteventura bring evidence of 5-8% and 10-20% of crustal assimilation, respectively  
282 (Thirlwall et al., 1997; Hoernle, 1998; Demény et al., 1998; Gurenko et al., 2006; Day et al., 2010), which  
283 could justify the lowering of their  $^3\text{He}/^4\text{He}$  values.

284 Magma ageing also can change the abundance of helium isotopes and can be invoked to explain the low  
285  $^3\text{He}/^4\text{He}$  ratios observed in magmatic rocks from the eastern Canary Islands. As discussed by several authors,  
286 when magma ponds in the crust for a long time, the  $^3\text{He}/^4\text{He}$  ratios eventually decrease due to the accumulation  
287 of radiogenic  $^4\text{He}$  over time (Torgersen and Jenkins, 1982; Hilton et al., 1993; Burnard, 2013). In the case of  
288 Gran Canaria, it is possible to estimate the production of radiogenic  $^4\text{He}$  in magmas based on the U and Th  
289 abundances reported in basaltic rocks (Ballentine and Burnard, 2002). Considering an average concentration  
290 of 0.8 ppm and 3.4 ppm for U and Th, respectively (Thirlwall et al., 1997), the quantity of  $^4\text{He}$  produced in  
291 Gran Canaria magmas would be  $8.93 \times 10^{-18}$  mol/g\*yr. Although no information about magma residence time  
292 has been reported in the literature, van den Bogaard et al. (1988) proposed an eruptive periodicity of 0.05 Ma,  
293 which is closely connected with periods of differentiation and recharge of magma reservoirs. Thus, assuming  
294 a starting Rc/Ra = 8, a  $^4\text{He}$  concentration of  $2.5 \times 10^{-12}$  mol/g (the maximum concentration reported in volcanic  
295 rocks in Canary Islands, Fig. 2) and the above  $^4\text{He}$  production rate, we conclude that a crustal residence time  
296 between 0.05 and 0.06 Ma is sufficient to lower the initial  $^3\text{He}/^4\text{He}$  to 6.96 Ra, which agrees well with the  
297 values reported for Gran Canaria basalts ( $\sim 6.69 \pm 0.46$  Ra).

298 We reiterate our interpretation is no alternative to and does not intend to dismiss earlier models (Hoernle et  
299 al., 1991; Simonsen et al., 2000; Gurenko et al., 2006) that emphasise the role of mantle heterogeneity. Any  
300 contribution of crustal He may, in fact, contribute to additionally lowering the  $^3\text{He}/^4\text{He}$  values of lavas derive  
301 from an already enriched (EM) mantle source. We argue that additional work on FI in mantle xenoliths is  
302 needed (especially in La Palma, Tenerife, Gran Canaria, Lanzarote, and Fuerteventura) in order to quantify  
303 better the relative roles played by crustal interactions and mantle heterogeneities (a continental lithospheric  
304 component in the mantle source) in this portion of the Canary Islands. Mantle xenoliths are indeed much better  
305 proxies of the source mantle than lavas, in which a role of shallow crustal processes is often more challenging  
306 to dismiss.

307

### 308 ***5.3. Recycled CO<sub>2</sub> in the mantle source***

309 Our results thus bring no evidence of a recycled crustal He component in the El Hierro mantle source. This  
310 contrasts with our El Hierro CO<sub>2</sub> isotopic measurements that, being the first FI results for Canary Islands,  
311 points to a  $^{13}\text{C}$ -enriched mantle source (Fig. 4). We find that both olivines and pyroxenes exhibit higher  $\delta^{13}\text{C}$   
312 values than the classical MORB range ( $-8\text{‰} < \delta^{13}\text{C} < -4\text{‰}$ ; Sano and Marty, 1995), and approaching those  
313 of crustal carbonate reservoirs (Marty and Jambon, 1987; Sano and Marty, 1995). Our mantle xenolith results  
314 are unique for the Canary Islands, as previous isotopic compositions of CO<sub>2</sub> ( $\delta^{13}\text{C}$ ) have only been obtained  
315 for volcanic gases and groundwaters (from La Palma and Tenerife) and for some carbonatites (from  
316 Fuerteventura) (see Table S1 and Fig. 4). In the remaining Islands, no  $\delta^{13}\text{C}$  information is available due to the  
317 lack of surface gas emissions and the technical challenges in extracting CO<sub>2</sub> from (and measuring  $\delta^{13}\text{C}$  in) FI  
318 in lavas.

319

320 The El Hierro FI results demonstrate a crustal C component in the source mantle, previously un-identified in  
321 volcanic gases/groundwater studies in the region (Fig. 4). When comparing our  $\delta^{13}\text{C}$  values with either Rc/Ra  
322 (Fig 4A) and CO<sub>2</sub>/ $^3\text{He}$  (Fig. 4B), the pyroxene-hosted FI fall along a MORB-Limestone mixing line, pointing  
323 to a carbonate component in the local mantle. For comparison, volcanic gases from La Palma and Tenerife  
324 exhibit CO<sub>2</sub>/ $^3\text{He}$  and  $\delta^{13}\text{C}$  values that, although consistent with a mixing MORB-Limestone (Fig. 4B), have

325 less extreme compositions, in which thus the crustal C contribution is much less manifest. Besides, in the case  
326 of groundwaters from Tenerife and La Palma, the low Rc/Ra and more negative  $\delta^{13}\text{C}$  values suggest the  
327 addition of crustal-derived radiogenic  $^4\text{He}$  and organic carbon, as well the fractionation of carbon during  $\text{CO}_2$   
328 dissolution in water (Fig. 4A).

329

330 The olivine-hosted El Hierro FI exhibit even more extreme  $^{13}\text{C}$ -rich compositions ( $\delta^{13}\text{C}$  values of  $-0.19\text{‰}$  and  
331  $+0.96\text{‰}$ ) (Fig. 4). Unlike pyroxenes from El Hierro and volcanic gases from Tenerife and La Palma, these  
332 unusually positive olivine results cannot result from a classical MORB-limestone mixing (Fig. 4A). In line  
333 with the HIMU affinity of the El Hierro mantle source (Day et al., 2010; Day and Hilton, 2011), we propose,  
334 instead, that this positive  $\delta^{13}\text{C}$  signature derives from the addition to the local mantle of recycled crustal carbon  
335 transported by old subducted altered oceanic crust (AOC) and/or oceanic lithosphere (OL) (Fig. 4). Recycled  
336 AOC and OL components are essential carriers of crustal carbon into the mantle during subduction (Li et al.,  
337 2019; Plank and Manning, 2019). This is because AOC and OL precipitate carbonates during hydrothermal  
338 alteration at mid-ocean ridges (Alt and Teagle, 1999; Alt et al., 2013). Li et al. (2019) and references therein  
339 report the existence of carbonates in AOC and OL with  $\delta^{13}\text{C}$  values as low as  $-24\text{‰}$  and as high as  $+10.3\text{‰}$ ,  
340 where the extremely positive  $\delta^{13}\text{C}$  values result from the inorganic reduction of  $\text{CO}_2$  to methane by either  
341 abiotic or biotic processes (Alt and Shanks, 2003) or microbial methanogenesis (Kenward et al., 2009). We  
342 show in Fig. 4 model binary mixing lines between MORB and AOC/OL, drawn by considering the range of  
343  $\delta^{13}\text{C}$  carbonate signatures observed in Li et al., (2019). In particular, from the dataset reported by Li et al.,  
344 (2019), we select the isotopic compositions of two carbonates contained in AOC and two carbonates contained  
345 in OL, being characterised by different ages. Carbonates in AOC and OL older than 85 Ma exhibit  $\delta^{13}\text{C}$  values  
346 as high as  $+3.5\text{‰}$  and  $+2.1\text{‰}$ , respectively, while carbonates in AOC and OL younger than 85 Ma exhibit  $\delta^{13}\text{C}$   
347 as high as  $+4.7\text{‰}$  and  $+10.9\text{‰}$ , respectively (Li et al., 2019). The Rc/Ra and  $\text{CO}_2/{}^3\text{He}$  compositions of the  
348 AOC/OL end-member are unfortunately undetermined. For the sake of illustration, these AOC/OL components  
349 are here assumed (Fig. 4) to have Rc/Ra and  $\text{CO}_2/{}^3\text{He}$  ratios corresponding to those of crustal limestones ( $0.01$   
350  $\text{Ra}$  and  $1.0 \times 10^{13}$ , respectively), which is likely to be very rough assumption as, for example,  $\text{CO}_2$  and He can  
351 undergo fractionation during eclogite formation and melting in the slab. Ultimately, the calculated mixing  
352 curves fit the  $\delta^{13}\text{C}$  values measured in olivines well, supporting the presence of C-rich fluids derived from

353 recycled AOC and/or OL in the mantle beneath El Hierro (Fig. 4). We caution, however, that the AOC / OL  
354 end-member can in fact sit in any position along the depicted mixing curve(s), so that (in the most extreme  
355 case) the olivines may have recorded the eclogitic component fully (e.g., with no dilution from the MORB).

356

357 The existence of a C-rich component underneath El Hierro is strongly supported by petrological and FI  
358 evidence on the same suite of mantle xenoliths (Oglialoro et al., 2017; Remigi et al., 2019; Colombo, 2020).

359 According to these authors, the presence of high-density CO<sub>2</sub>-N<sub>2</sub> FI and interstitial microveins composed of  
360 silicate glass (andesitic-trachytic in composition) and carbonate droplets (calcite and Mg-calcite) are evidence  
361 of mantle metasomatism caused by deep infiltration of volatile-rich, carbonate-silicate melts, likely derived  
362 from carbonated-eclogite melting at high pressure (Remigi et al., 2019). Mantle metasomatism by C-rich  
363 (either carbonatitic or carbonate-silicate) melts underneath the Canary Islands has recurrently been described  
364 earlier at El Hierro (Neumann, 1991) and in nearby islands (Frezzotti et al., 2002a, 2002b; Neumann, 2004).

365 The timing of the paleo-subduction event(s) of AOC-OL recycling is difficult to determine. However, it may  
366 coincide with fossil subduction(s) (1-2 Ga old) responsible for the recycling of old oceanic crust and  
367 lithosphere, invoked to support the HIMU mantle signature underneath El Hierro and La Palma (e.g., Hoernle  
368 et al., 1991; Gurenko et al., 2006; Day et al., 2010; Day and Hilton, 2011, 2020).

369

## 370 **6. CONCLUDING REMARKS**

371 We have reported on the first FI-based  $\delta^{13}\text{C}$  evidence for a recycled carbon component in the source mantle  
372 feeding El Hierro volcanism. To the best of our knowledge, this is the first direct isotopic evidence for C-rich  
373 metasomatic melts having modified the composition of the local mantle, perhaps in response to the past (old,  
374 1-2 Ga old) oceanic subduction events that are implicated by the HIMU affinity of the mantle/magmas.

375 Pyroxene- and olivine-hosted FI record such infiltration of crustal C-rich melts in the mantle but exhibit  
376 different extents of  $^{13}\text{C}$  enrichment. The cause of this isotopic dissimilarity in the El Hierro xenolith mineral  
377 suite is unknown. Some C isotopic fractionation may occur during mineral-melt-exsolved fluid interaction  
378 deep in the mantle.

379 He, Ar and Ne systematics in our xenoliths confirm a depleted mantle (DMM-type) signature for the  
380 lithospheric mantle beneath El Hierro, in agreement with  $^3\text{He}/^4\text{He}$  signatures previously reported for  
381 groundwater and lava-hosted FI. This helium isotopic signature of El Hierro persists in time, suggesting a  
382 homogeneity in the local mantle composition at least over the last million years. This MORB-like signature  
383 argues against a primordial He source affecting the local lithospheric mantle and suggests a marginal He slab  
384 transport during past subduction events. The more radiogenic He signature in the eastern Canary Islands may  
385 reflect a combination of an EM source, magma ageing and/or assimilation of radiogenic He upon magma  
386 ascent in the crust.

387

## 388 **ACKNOWLEDGMENTS**

389 This paper is part of the PhD (XXXIV cycle) of Andres Libardo Sandoval Velasquez at the University of  
390 Palermo. This study also received funding from Italian MIUR (Grant N. 2017LMNLAW). We are grateful to  
391 Mariano Tantillo and Mariagrazia Misseri for helping in sample preparation, the isotope analysis of noble  
392 gases and the  $\text{CO}_2$  extraction from fluid inclusions performed in the noble gas laboratory of INGV-Palermo.  
393 We also thank Ygor Oliveri and Giorgio Capasso for their help in the  $\text{CO}_2$  isotopic analysis carried out in the  
394 INGV-Palermo stable isotopes laboratory.

395

## 396 **REFERENCES**

397 Abratis, M., Schmincke, H.-U., Hansteen, T., 2002. Composition and evolution of submarine  
398 volcanic rocks from the central and western Canary Islands. *Int. J. Earth Sci.* 91, 562–582.  
399 <https://doi.org/10.1007/s00531-002-0286-7>

400 Admunsen, H.E.F., 1987. Peridotite xenoliths from Gran Canaria, Canary Islands; evidence for  
401 metasomatic processes and partial melting in the lower oceanic crust. *Neues Jahrb. Für Mineral.*  
402 *Abh.* 156, 121–140.

403 Aiuppa, A., Fischer, T.P., Plank, T., Robidoux, P., Di Napoli, R., 2017. Along-arc, inter-arc and  
404 arc-to-arc variations in volcanic gas  $\text{CO}_2/\text{ST}$  ratios reveal dual source of carbon in arc volcanism.  
405 *Earth-Sci. Rev.* 168, 24–47. <https://doi.org/10.1016/j.earscirev.2017.03.005>

406 Alt, J.C., Schwarzenbach, E.M., Früh-Green, G.L., Shanks, W.C., Bernasconi, S.M., Garrido, C.J.,  
407 Crispini, L., Gaggero, L., Padrón-Navarta, J.A., Marchesi, C., 2013. The role of serpentinites in  
408 cycling of carbon and sulfur: Seafloor serpentinitization and subduction metamorphism. *Lithos*,

409 Serpentinites from mid-oceanic ridges to subduction 178, 40–54.  
410 <https://doi.org/10.1016/j.lithos.2012.12.006>

411 Alt, J.C., Shanks, W.C., 2003. Serpentinization of abyssal peridotites from the MARK area, Mid-  
412 Atlantic Ridge: sulfur geochemistry and reaction modeling. *Geochim. Cosmochim. Acta* 67, 641–  
413 653. [https://doi.org/10.1016/S0016-7037\(02\)01142-0](https://doi.org/10.1016/S0016-7037(02)01142-0)

414 Alt, J.C., Teagle, D.A.H., 1999. The uptake of carbon during alteration of ocean crust. *Geochim.*  
415 *Cosmochim. Acta* 63, 1527–1535. [https://doi.org/10.1016/S0016-7037\(99\)00123-4](https://doi.org/10.1016/S0016-7037(99)00123-4)

416 Anguita, F., Hernán, F., 2000. The Canary Islands origin: a unifying model. *J. Volcanol. Geotherm.*  
417 *Res.* 103, 1–26. [https://doi.org/10.1016/S0377-0273\(00\)00195-5](https://doi.org/10.1016/S0377-0273(00)00195-5)

418 Anguita, F., Hernan, F., 1975. A propagating fracture model versus a hot spot origin for the Canary  
419 islands. *Earth Planet. Sci. Lett.* 27, 11–19. [https://doi.org/10.1016/0012-821X\(75\)90155-7](https://doi.org/10.1016/0012-821X(75)90155-7)

420 Araña, V., Ortiz, R., 1991. The Canary Islands: Tectonics, Magmatism and Geodynamic  
421 Framework, in: Kampunzu, A.B., Lubala, R.T. (Eds.), *Magmatism in Extensional Structural*  
422 *Settings*. Springer Berlin Heidelberg, Berlin, Heidelberg, pp. 209–249. [https://doi.org/10.1007/978-](https://doi.org/10.1007/978-3-642-73966-8_9)  
423 [3-642-73966-8\\_9](https://doi.org/10.1007/978-3-642-73966-8_9)

424 Ballentine, C.J., Burnard, P.G., 2002. Production, Release and Transport of Noble Gases in the  
425 Continental Crust. *Rev. Mineral. Geochem.* 47, 481–538. <https://doi.org/10.2138/rmg.2002.47.12>

426 Boudoire, G., Rizzo, A.L., Di Muro, A., Grassa, F., Liuzzo, M., 2018. Extensive CO<sub>2</sub> degassing in  
427 the upper mantle beneath oceanic basaltic volcanoes: First insights from Piton de la Fournaise  
428 volcano (La Réunion Island). *Geochim. Cosmochim. Acta* 235, 376–401.  
429 <https://doi.org/10.1016/j.gca.2018.06.004>

430 Broadley, M.W., Ballentine, C.J., Chavrit, D., Dallai, L., Burgess, R., 2016. Sedimentary halogens  
431 and noble gases within Western Antarctic xenoliths: Implications of extensive volatile recycling to  
432 the sub continental lithospheric mantle. *Geochim. Cosmochim. Acta* 176, 139–156.  
433 <https://doi.org/10.1016/j.gca.2015.12.013>

434 Burnard, P. (Ed.), 2013. *The noble gases as geochemical tracers, Advances in isotope geochemistry.*  
435 Springer, Heidelberg ; New York.

436 Carnevale, G., Caracausi, A., Correale, A., Italiano, L., Rotolo, S., 2021. An Overview of the  
437 Geochemical Characteristics of Oceanic Carbonatites: New Insights from Fuerteventura  
438 Carbonatites (Canary Islands). *Minerals* 11, 203. <https://doi.org/10.3390/min11020203>

439 Carracedo, J.C., Day, S., Guillou, H., Rodríguez Badiola, E., Canas, J.A., Pérez Torrado, F.J., 1998.  
440 Hotspot volcanism close to a passive continental margin: the Canary Islands. *Geol. Mag.* 135, 591–  
441 604. <https://doi.org/10.1017/S0016756898001447>

442 Clarke, W.B., Jenkins, W.J., Top, Z., 1976. Determination of tritium by mass spectrometric  
443 measurement of <sup>3</sup>He. *Int. J. Appl. Radiat. Isot.* 27, 515–522. [https://doi.org/10.1016/0020-](https://doi.org/10.1016/0020-708X(76)90082-X)  
444 [708X\(76\)90082-X](https://doi.org/10.1016/0020-708X(76)90082-X)

445 Colombo, E., 2020. Petrological study of peridotite xenoliths of El Hierro island: characterization of  
446 the lithospheric mantle beneath the Canary Islands (Spain) (Master’s Thesis). University of Milano-  
447 Bicocca, Milan.

448 Correale, A., Paonita, A., Rizzo, A., Grassa, F., Martelli, M., 2015. The carbon-isotope signature of  
449 ultramafic xenoliths from the Hyblean Plateau (southeast Sicily, Italy): Evidence of mantle  
450 heterogeneity. *Geochem. Geophys. Geosystems* 16, 600–611.  
451 <https://doi.org/10.1002/2014GC005656>

452 Correale, A., Pelorosso, B., Rizzo, A.L., Coltorti, M., Italiano, F., Bonadiman, C., Giacomoni, P.P.,  
453 2019. The nature of the West Antarctic Rift System as revealed by noble gases in mantle minerals.  
454 *Chem. Geol.* 524, 104–118. <https://doi.org/10.1016/j.chemgeo.2019.06.020>

455 Dasgupta, R., Hirschmann, M.M., 2010. The deep carbon cycle and melting in Earth's interior.  
456 *Earth Planet. Sci. Lett.* 298, 1–13. <https://doi.org/10.1016/j.epsl.2010.06.039>

457 Dasgupta, R., Jackson, M.G., Lee, C.-T.A., 2010. Major element chemistry of ocean island basalts  
458 — Conditions of mantle melting and heterogeneity of mantle source. *Earth Planet. Sci. Lett.* 289,  
459 377–392. <https://doi.org/10.1016/j.epsl.2009.11.027>

460 Day, J.M.D., Barry, P.H., Hilton, D.R., Burgess, R., Pearson, D.G., Taylor, L.A., 2015. The helium  
461 flux from the continents and ubiquity of low-3He/4He recycled crust and lithosphere. *Geochim.*  
462 *Cosmochim. Acta* 153, 116–133. <https://doi.org/10.1016/j.gca.2015.01.008>

463 Day, J.M.D., Hilton, D.R., 2020. Heterogeneous mantle-derived helium isotopes in the  
464 Canary Islands and other ocean islands. *Geology*. <https://doi.org/10.1130/G47676.1>

465 Day, J.M.D., Hilton, D.R., 2011. Origin of 3He/4He ratios in HIMU-type basalts constrained from  
466 Canary Island lavas. *Earth Planet. Sci. Lett.* 305, 226–234.  
467 <https://doi.org/10.1016/j.epsl.2011.03.006>

468 Day, J.M.D., Pearson, D.G., Macpherson, C.G., Lowry, D., Carracedo, J.C., 2010. Evidence for  
469 distinct proportions of subducted oceanic crust and lithosphere in HIMU-type mantle beneath El  
470 Hierro and La Palma, Canary Islands. *Geochim. Cosmochim. Acta* 74, 6565–6589.  
471 <https://doi.org/10.1016/j.gca.2010.08.021>

472 Deines, P., 2002. The carbon isotope geochemistry of mantle xenoliths. *Earth-Sci. Rev.* 58, 247–  
473 278. [https://doi.org/10.1016/S0012-8252\(02\)00064-8](https://doi.org/10.1016/S0012-8252(02)00064-8)

474 Demény, A., Ahijado, A., Casillas, R., Vennemann, T.W., 1998. Crustal contamination and  
475 fluid/rock interaction in the carbonatites of Fuerteventura (Canary Islands, Spain): a C, O, H isotope  
476 study. *Lithos* 44, 101–115. [https://doi.org/10.1016/S0024-4937\(98\)00050-4](https://doi.org/10.1016/S0024-4937(98)00050-4)

477 Demény, A., Dallai, L., Frezzotti, M.-L., Vennemann, T.W., Embey-Isztin, A., Dobosi, G., Nagy,  
478 G., 2010. Origin of CO<sub>2</sub> and carbonate veins in mantle-derived xenoliths in the Pannonian Basin.  
479 *Lithos* 117, 172–182. <https://doi.org/10.1016/j.lithos.2010.02.013>

480 Duncan, M.S., Dasgupta, R., 2017. Rise of Earth's atmospheric oxygen controlled by efficient  
481 subduction of organic carbon. *Nat. Geosci.* 10, 387–392. <https://doi.org/10.1038/ngeo2939>

482 Frezzotti, M.L., Andersen, T., Neumann, E.-R., Simonsen, S.L., 2002a. Carbonatite melt–CO<sub>2</sub> fluid  
483 inclusions in mantle xenoliths from Tenerife, Canary Islands: a story of trapping, immiscibility and  
484 fluid–rock interaction in the upper mantle. *Lithos* 64, 77–96. [https://doi.org/10.1016/S0024-4937\(02\)00178-0](https://doi.org/10.1016/S0024-4937(02)00178-0)

485

486 Frezzotti, M.L., Ferrando, S., Tecce, F., Castelli, D., 2012b. Water content and nature of solutes in  
487 shallow-mantle fluids from fluid inclusions. *Earth Planet. Sci. Lett.* 351–352, 70–83.  
488 <https://doi.org/10.1016/j.epsl.2012.07.023>

489 Frezzotti, M.-L., Touret, J.L.R., 2014. CO<sub>2</sub>, carbonate-rich melts, and brines in the mantle. *Geosci.*  
490 *Front.* 5, 697–710. <https://doi.org/10.1016/j.gsf.2014.03.014>

491 Frezzotti, M.-L., Touret, J.L.R., Neumann, E.-R., 2002b. Ephemeral carbonate melts in the upper  
492 mantle: carbonate-silicate immiscibility in microveins and inclusions within spinel peridotite  
493 xenoliths, La Gomera, Canary Islands. *Eur. J. Mineral.* 14, 891–904. [https://doi.org/10.1127/0935-](https://doi.org/10.1127/0935-1221/2002/0014-0891)  
494 [1221/2002/0014-0891](https://doi.org/10.1127/0935-1221/2002/0014-0891)

495 Gautheron, C., Moreira, M., 2002. Helium signature of the subcontinental lithospheric mantle. *Earth*  
496 *Planet. Sci. Lett.* 199, 39–47. [https://doi.org/10.1016/S0012-821X\(02\)00563-0](https://doi.org/10.1016/S0012-821X(02)00563-0)

497 Gennaro, M.E., Grassa, F., Martelli, M., Renzulli, A., Rizzo, A.L., 2017. Carbon isotope  
498 composition of CO<sub>2</sub>-rich inclusions in cumulate-forming mantle minerals from Stromboli volcano  
499 (Italy). *J. Volcanol. Geotherm. Res.* 346, 95–103. <https://doi.org/10.1016/j.jvolgeores.2017.04.001>

500 Graham, D.W., 2002. Noble Gas Isotope Geochemistry of Mid-Ocean Ridge and Ocean Island  
501 Basalts: Characterization of Mantle Source Reservoirs. *Rev. Mineral. Geochem.* 47, 247–317.  
502 <https://doi.org/10.2138/rmg.2002.47.8>

503 Gurenko, A.A., Hoernle, K.A., Hauff, F., Schmincke, H.-U., Han, D., Miura, Y.N., Kaneoka, I.,  
504 2006. Major, trace element and Nd–Sr–Pb–O–He–Ar isotope signatures of shield stage lavas from  
505 the central and western Canary Islands: Insights into mantle and crustal processes. *Chem. Geol.*  
506 233, 75–112. <https://doi.org/10.1016/j.chemgeo.2006.02.016>

507 Hammouda, T., Keshav, S., 2015. Melting in the mantle in presence of carbon; review of  
508 experiments and discussion on the origin of carbonatites. *Chem. Geol.* 418.  
509 <https://doi.org/10.1016/j.chemgeo.2015.05.018>

510 Hazen, R., Downs, R., Kah, L., Sverjensky, D., 2013. Carbon Mineral Evolution. *Rev. Mineral.*  
511 *Geochem.* 75, 79–107. <https://doi.org/10.2138/rmg.2013.75.4>

512 Hilton, D.R., Hammerschmidt, K., Teufel, S., Friedrichsen, H., 1993. Helium isotope characteristics  
513 of Andean geothermal fluids and lavas. *Earth Planet. Sci. Lett.* 120, 265–282.  
514 [https://doi.org/10.1016/0012-821X\(93\)90244-4](https://doi.org/10.1016/0012-821X(93)90244-4)

515 Hilton, D.R., Macpherson, C.G., Elliott, T.R., 2000. Helium isotope ratios in mafic phenocrysts and  
516 geothermal fluids from La Palma, the Canary Islands (Spain): implications for HIMU mantle  
517 sources. *Geochim. Cosmochim. Acta* 64, 2119–2132. [https://doi.org/10.1016/S0016-](https://doi.org/10.1016/S0016-7037(00)00358-6)  
518 [7037\(00\)00358-6](https://doi.org/10.1016/S0016-7037(00)00358-6)

519 Hoernle, K., 1998. Geochemistry of Jurassic Oceanic Crust beneath Gran Canaria (Canary Islands):  
520 Implications for Crustal Recycling and Assimilation. *J. Petrol. - J Pet.* 39, 859–880.  
521 <https://doi.org/10.1093/petrology/39.5.859>

522 Hoernle, K., Schmincke, H.-U., 1993. The Role of Partial Melting in the 15-Ma Geochemical  
523 Evolution of Gran Canaria: A Blob Model for the Canary Hotspot. *J. Petrol.* 34, 599–626.  
524 <https://doi.org/10.1093/petrology/34.3.599>

525 Hoernle, K., Tilton, G., Schmincke, H.-U., 1991. SrNdPb isotopic evolution of Gran Canaria:  
526 Evidence for shallow enriched mantle beneath the Canary Islands. *Earth Planet. Sci. Lett.* 106, 44–  
527 63. [https://doi.org/10.1016/0012-821X\(91\)90062-M](https://doi.org/10.1016/0012-821X(91)90062-M)



528 Hoernle, K., Zhang, Y.-S., Graham, D., 1995. Seismic and geochemical evidence for large-scale  
529 mantle upwelling beneath the eastern Atlantic and western and central Europe. *Nature* 374, 34–39.  
530 <https://doi.org/10.1038/374034a0>

531 Hofmann, A., 2003. Sampling Mantle Heterogeneity through Oceanic Basalts: Isotopes and Trace  
532 Elements. *Mantle Core* 61-101 2003 2. <https://doi.org/10.1016/B0-08-043751-6/02123-X>

533 Hofmann, A.W., 1997. Mantle geochemistry: the message from oceanic volcanism. *Nature* 385,  
534 219–229. <https://doi.org/10.1038/385219a0>

535 Holik, J.S., Rabinowitz, P.D., Austin, J.A., 1991. Effects of Canary hotspot volcanism on structure  
536 of oceanic crust off Morocco. *J. Geophys. Res.* 96, 12039. <https://doi.org/10.1029/91JB00709>

537 Jackson, M., Dasgupta, R., 2008. Compositions of HIMU, EM1, and EM2 from global trends  
538 between radiogenic isotopes and major elements in ocean island basalts. *Earth Planet. Sci. Lett.*  
539 276, 175–186. <https://doi.org/10.1016/j.epsl.2008.09.023>

540 Kenward, P.A., Goldstein, R.H., González, L.A., Roberts, J.A., 2009. Precipitation of low-  
541 temperature dolomite from an anaerobic microbial consortium: the role of methanogenic Archaea.  
542 *Geobiology* 7, 556–565. <https://doi.org/10.1111/j.1472-4669.2009.00210.x>

543 Kobayashi, M., Sumino, H., Burgess, R., Nakai, S., Iizuka, T., Nagao, J., Kagi, H., Nakamura, M.,  
544 Takahashi, E., Kogiso, T., Ballentine, C.J., 2019. Halogen Heterogeneity in the Lithosphere and  
545 Evolution of Mantle Halogen Abundances Inferred From Intraplate Mantle Xenoliths. *Geochem.*  
546 *Geophys. Geosystems* 20, 952–973. <https://doi.org/10.1029/2018GC007903>

547 Kurz, M.D., 1986. Cosmogenic helium in a terrestrial igneous rock. *Nature* 320, 435–439.  
548 <https://doi.org/10.1038/320435a0>

549 Li, K., Li, L., Pearson, D.G., Stachel, T., 2019. Diamond isotope compositions indicate altered  
550 igneous oceanic crust dominates deep carbon recycling. *Earth Planet. Sci. Lett.* 516, 190–201.  
551 <https://doi.org/10.1016/j.epsl.2019.03.041>

552 Martin, L.A.J., Hermann, J., 2018. Experimental Phase Relations in Altered Oceanic Crust:  
553 Implications for Carbon Recycling at Subduction Zones. *J. Petrol.* 59, 299–320.  
554 <https://doi.org/10.1093/petrology/egy031>

555 Martínez-Arevalo, C., Mancilla, F. de L., Helffrich, G., García, A., 2013. Seismic evidence of a  
556 regional sublithospheric low velocity layer beneath the Canary Islands. *Tectonophysics* 608, 586–  
557 599. <https://doi.org/10.1016/j.tecto.2013.08.021>

558 Marty, B., Jambon, A., 1987. C3He in volatile fluxes from the solid Earth: implications for carbon  
559 geodynamics. *Earth Planet. Sci. Lett.* 83, 16–26. [https://doi.org/10.1016/0012-821X\(87\)90047-1](https://doi.org/10.1016/0012-821X(87)90047-1)

560 Montelli, R., 2004. Finite-Frequency Tomography Reveals a Variety of Plumes in the Mantle.  
561 *Science* 303, 338–343. <https://doi.org/10.1126/science.1092485>

562 Neumann, E.-R., 2004. The Evolution of the Upper Mantle beneath the Canary Islands: Information  
563 from Trace Elements and Sr isotope Ratios in Minerals in Mantle Xenoliths. *J. Petrol.* 45, 2573–  
564 2612. <https://doi.org/10.1093/petrology/egh063>

565 Neumann, E.-R., 1991. Ultramafic and mafic xenoliths from Hierro, Canary Islands: evidence for  
566 melt infiltration in the upper mantle. *Contrib. Mineral. Petrol.* 106, 236–252.  
567 <https://doi.org/10.1007/BF00306436>

- 568 Neumann, E.-R., Wulff-Pedersen, E., 1997. The Origin of Highly Silicic Glass in Mantle Xenoliths  
569 from the Canary Islands. *J. Petrol.* 38, 1513–1539. <https://doi.org/10.1093/petroj/38.11.1513>
- 570 Oglialoro, E., Frezzotti, M.L., Ferrando, S., Tiraboschi, C., Principe, C., GropPELLI, G., Villa, I.M.,  
571 2017. Lithospheric magma dynamics beneath the El Hierro Volcano, Canary Islands: insights from  
572 fluid inclusions. *Bull. Volcanol.* 79, 70. <https://doi.org/10.1007/s00445-017-1152-6>
- 573 Ozima, M., Podosek, F.A., 2001. *Noble Gas Geochemistry*, 2nd ed. Cambridge University Press,  
574 Cambridge. <https://doi.org/10.1017/CBO9780511545986>
- 575 Padrón, E., Pérez, N.M., Hernández, P.A., Sumino, H., Melián, G.V., Barrancos, J., Nolasco, D.,  
576 Padilla, G., Dionis, S., Rodríguez, F., Hernández, Í., Calvo, D., Peraza, M.D., Nagao, K., 2013.  
577 Diffusive helium emissions as a precursory sign of volcanic unrest. *Geology* 41, 539–542.  
578 <https://doi.org/10.1130/G34027.1>
- 579 Pearson, D.G., Canil, D., Shirey, S.B., 2014. Mantle Samples Included in Volcanic Rocks, in:  
580 *Treatise on Geochemistry*. Elsevier, pp. 169–253. [https://doi.org/10.1016/B978-0-08-095975-](https://doi.org/10.1016/B978-0-08-095975-7.00216-3)  
581 [7.00216-3](https://doi.org/10.1016/B978-0-08-095975-7.00216-3)
- 582 Pérez, N.M., Nakai, S., Wakita, H., Hernández, P.A., Salazar, J.M., 1996. Helium-3 emission in and  
583 around Teide Volcano, Tenerife, Canary Islands, Spain. *Geophys. Res. Lett.* 23, 3531–3534.  
584 <https://doi.org/10.1029/96GL03470>
- 585 Pérez, N.M., Nakai, S., Wakita, H., Sano, Y., Williams, S.N., 1994.  $^3\text{He}/^4\text{He}$  Isotopic Ratios in  
586 Volcanic-Hydrothermal Discharges from the Canary Islands, Spain: Implications on the Origin of  
587 the Volcanic Activity. *Mineral. Mag.* 58, 709–710. <https://doi.org/10.1180/minmag.1994.58A.2.107>
- 588 Plank, T., Manning, C.E., 2019. Subducting carbon. *Nature* 574, 343–352.  
589 <https://doi.org/10.1038/s41586-019-1643-z>
- 590 Regier, M.E., Pearson, D.G., Stachel, T., Luth, R.W., Stern, R.A., Harris, J.W., 2020. The  
591 lithospheric-to-lower-mantle carbon cycle recorded in superdeep diamonds. *Nature* 585, 234–238.  
592 <https://doi.org/10.1038/s41586-020-2676-z>
- 593 Remigi, S., Frezzotti, M.L., Ferrando, S., 2019. Generation of CO<sub>2</sub> - SO<sub>2</sub> fluxes in the lithospheric  
594 mantle beneath El Hierro (Canary Islands) on metasomatic reactions of carbonate-rich silicate  
595 melts, Intervento presentato a: ECROFI, Budapest. Università di Milano Bicocca, Milan.
- 596 Rizzo, A.L., Pelorosso, B., Coltorti, M., Ntaflos, T., Bonadiman, C., Matusiak-Małek, M., Italiano,  
597 F., Bergonzoni, G., 2018. Geochemistry of Noble Gases and CO<sub>2</sub> in Fluid Inclusions From  
598 Lithospheric Mantle Beneath Wilcza Góra (Lower Silesia, Southwest Poland). *Front. Earth Sci.* 6,  
599 215. <https://doi.org/10.3389/feart.2018.00215>
- 600 Sano, Y., Marty, B., 1995. Origin of carbon in Fumarolic gas from island arcs. *Chem. Geol.* 119,  
601 265–274. [https://doi.org/10.1016/0009-2541\(94\)00097-R](https://doi.org/10.1016/0009-2541(94)00097-R)
- 602 Schmincke, H.-U., 1982. Volcanic and Chemical Evolution of the Canary Islands, in: von Rad, U.,  
603 Hinz, K., Sarnthein, M., Seibold, E. (Eds.), *Geology of the Northwest African Continental Margin*.  
604 Springer Berlin Heidelberg, Berlin, Heidelberg, pp. 273–306. [https://doi.org/10.1007/978-3-642-](https://doi.org/10.1007/978-3-642-68409-8_12)  
605 [68409-8\\_12](https://doi.org/10.1007/978-3-642-68409-8_12)
- 606 Siena, F., Beccaluva, L., Coltorti, M., Marchesi, S., Morra, V., 1991. Ridge to Hot-Spot Evolution  
607 of the Atlantic Lithospheric Mantle: Evidence from Lanzarote Peridotite Xenoliths (Canary

- 608 Islands). *J. Petrol. Special\_Volume*, 271–290.  
609 [https://doi.org/10.1093/petrology/Special\\_Volume.2.271](https://doi.org/10.1093/petrology/Special_Volume.2.271)
- 610 Simonsen, S., Neumann, E.-R., Seim, K., 2000. Sr–Nd–Pb isotope and trace-element geochemistry  
611 evidence for a young HIMU source and assimilation at Tenerife (Canary Island). *J. Volcanol.*  
612 *Geotherm. Res. - J VOLCANOL GEOTHERM RES* 103, 299–312. [https://doi.org/10.1016/S0377-](https://doi.org/10.1016/S0377-0273(00)00228-6)  
613 [0273\(00\)00228-6](https://doi.org/10.1016/S0377-0273(00)00228-6)
- 614 Sobolev, A., Hofmann, A., Kuzmin, D., Yaxley, G., Arndt, N., Chung, S.-L., Danyushevsky, L.,  
615 Elliott, T., Frey, F., Garcia, M., Gurenko, A., Kamenetsky, V., Kerr, A., Krivolutsкая, N.,  
616 Matvienkov, V., Nikogosian, I., Rocholl, A., Sigurdsson, I., Sushchevskaya, N., Teklay, M., 2007.  
617 The Amount of Recycled Crust in Sources of Mantle-Derived Melts. *Science* 316, 412–7.  
618 <https://doi.org/10.1126/science.1138113>
- 619 Thirlwall, M.F., Jenkins, C., Vroon, P.Z., Matthey, D.P., 1997. Crustal interaction during  
620 construction of ocean islands: Pb-Sr-Nd-O isotope geochemistry of the shield basalts of Gran  
621 Canaria, Canary Islands. *Chem. Geol.* 135, 233–262. [https://doi.org/10.1016/S0009-](https://doi.org/10.1016/S0009-2541(96)00118-0)  
622 [2541\(96\)00118-0](https://doi.org/10.1016/S0009-2541(96)00118-0)
- 623 Torgersen, T., Jenkins, W.J., 1982. Helium isotopes in geothermal systems: Iceland, The Geysers,  
624 Raft River and Steamboat Springs. *Geochim. Cosmochim. Acta* 46, 739–748.  
625 [https://doi.org/10.1016/0016-7037\(82\)90025-4](https://doi.org/10.1016/0016-7037(82)90025-4)
- 626 Troll, V.R., Carracedo, J.C., 2016. *The Geology of the Canary Islands*. Elsevier.  
627 <https://doi.org/10.1016/C2015-0-04268-X>
- 628 van den Bogaard, P., 2013. The origin of the Canary Island Seamount Province - New ages of old  
629 seamounts. *Sci. Rep.* 3, 2107. <https://doi.org/10.1038/srep02107>
- 630 van den Bogaard, P., Schmincke, H.-U., Freundt, A., Hall, C.M., York, D., 1988. Eruption ages and  
631 magma supply rates during the miocene evolution of Gran Canaria: Single-crystal  $^{40}\text{Ar}/^{39}\text{Ar}$  laser  
632 ages. *Naturwissenschaften* 75, 616–617. <https://doi.org/10.1007/BF00366475>

633

634

635

## Figure Captions

636 **Figure 1.** The Canary Islands archipelago and sampling locality in El Julan Cliff Valley at El Hierro. Modified  
637 from Anguita and Hernán (2000), Oglialoro et al. (2017) and Day and Hilton (2020).  $^3\text{He}/^4\text{He}$  and  $\delta^{13}\text{C}$  values  
638 are from Tables 1 and S3. Ages in Ma represent the maximum ages reported in lavas for each Island (see Day  
639 et al., 2010). The path of the Canary hotspot was traced based on Holik et al. (1991) and Carracedo et al.  
640 (1998).

641 **Figure 2.**  $^4\text{He}$  vs Rc/Ra ratios ( $^3\text{He}/^4\text{He}$  ratio corrected for atmospheric contamination) measured in FI. MORB  
642 range is reported at Rc/Ra =  $8 \pm 1$  (Graham, 2002). White symbols are lava phenocrysts, the outline colours  
643 represent the island where the sample comes from (see legend). Purple asterisks represent the bulk  $^4\text{He}$   
644 concentrations and Rc/Ra values measured in ultramafic xenoliths from Lanzarote (see Table S1). A) The  
645 dotted blue line represents the maximum  $^3\text{He}/^4\text{He}$  ratio reported in groundwater samples during the volcanic  
646 unrest of 2012 at El Hierro (Padrón et al., 2013). B) An arbitrary cut-off value is proposed at  $9.0 \times 10^{-14}$  mol/g  
647 (see section SM3).

648 **Figure 3. A)** Histogram of filtered data, the resulting Rc/Ra values were classified in 11 different classes. An  
649 arbitrary cut-off value is proposed at 5 samples per class. Detailed description of data filtering is presented in  
650 SM3. **B)** Age vs Rc/Ra ratios ( $^3\text{He}/^4\text{He}$  corrected for atmospheric contamination) after data filtering. We  
651 plotted the year in which surface gases were sampled (bubbling gas, fumaroles and groundwater) and the age  
652 of the outcrop in the case of FI. **C)** Variability of Rc/Ra ratios along the Canarian archipelago. In the upper  
653 part of the graph, we designed the thickness of the oceanic crust beneath the Canary Islands based on the  
654 seismic information presented by Martinez-Arevalo et al. (2013). EH: El Hierro, LP: La Palma, LG: La  
655 Gomera, T: Tenerife, Ft: Fuerteventura, La: Lanzarote.

656 **Figure 4. A)**  $\delta^{13}\text{C}$  vs Rc/Ra ( $^3\text{He}/^4\text{He}$  corrected for atmospheric contamination). Dotted black lines are binary  
657 mixing curves between two endmembers: 1) Limestone at  $\delta^{13}\text{C} = -1\text{‰}$  and  $1\text{‰}$  and Rc/Ra = 0.01 and 2) MORB-  
658 like upper mantle at  $\delta^{13}\text{C} = -4\text{‰}$  and Rc/Ra = 7.45. The yellow square represents the variability of fumarolic  
659 samples from El Teide (Tenerife). **B)**  $\delta^{13}\text{C}$  vs  $\text{CO}_2/^3\text{He}$ . Dotted black lines are binary mixing between two  
660 endmembers: 1) Limestone at  $\delta^{13}\text{C} = -1\text{‰}$  and  $+1\text{‰}$  and  $\text{CO}_2/^3\text{He} = 10^{-13}$  and 2) MORB-like upper mantle at  
661  $\delta^{13}\text{C} = -4\text{‰}$  and  $\text{CO}_2/^3\text{He} = 1.00 \times 10^{-9}$  and  $2.00 \times 10^{-9}$ . Detailed description of MORB-AOC and MORB-OL  
662 binary mixing curves is presented in section 5.3. The histogram shows the number of samples (AOC-OL)  
663 reported for each  $\delta^{13}\text{C}$  class;  $\delta^{13}\text{C}$  values measured in AOC and OL were obtained from Li et al. (2019).

**Table 1.** Noble gas and CO<sub>2</sub> compositions of FI hosted in El Hierro mantle xenoliths. Concentrations of noble gases isotopes, CO<sub>2</sub> and N<sub>2</sub> are reported in mol/g. <sup>A</sup> First estimation of CO<sub>2</sub> contents in FI during noble gas analysis; <sup>B</sup> CO<sub>2</sub> contents and CO<sub>2</sub>/<sup>3</sup>He ratios measured from the glass line after CO<sub>2</sub> isotopic determinations. Reported errors are 2σ uncertainties.

Sample	Mineral	Rock type	ID (Ogialoro et al., 2017; Colombo, 2020)	Weight (g)	<sup>3</sup> He	<sup>4</sup> He	<sup>20</sup> Ne	<sup>21</sup> Ne	<sup>22</sup> Ne	CO <sub>2</sub> <sup>A</sup>	N <sub>2</sub> * <sup>C</sup>	<sup>40</sup> Ar	<sup>36</sup> Ar	<sup>40</sup> Ar* <sup>D</sup>	<sup>4</sup> He/ <sup>20</sup> Ne	<sup>4</sup> He/ <sup>40</sup> Ar*	<sup>4</sup> He/CO <sub>2</sub>
1.1	Ol	Sp Lherzolite	XML3	0.52644	1.28E-17	1.28E-12	5.67E-15	1.70E-17	5.65E-16	2.68E-08	4.73E-10	9.72E-12	2.35E-15	9.03E-12	225.9	0.14	4.78E-05
1.1	Opx	Sp Lherzolite	XML3	0.12869	2.48E-18	4.03E-13	6.74E-15	2.14E-17	6.82E-16	1.65E-08	3.29E-09	7.26E-12	2.66E-15	6.48E-12	59.8	0.06	2.45E-05
1.1	Cpx	Sp Lherzolite	XML3	0.08996	1.29E-18	1.58E-13	8.39E-15	2.56E-17	8.53E-16	7.70E-08	9.66E-09	6.27E-11	1.18E-14	5.92E-11	18.9	0.003	2.06E-06
1.15	Ol	Sp Harzburgite	XML11	0.51344	3.73E-17	3.60E-12	1.13E-14	3.35E-17	1.13E-15	8.45E-08	4.11E-10	6.09E-12	2.33E-15	5.41E-12	317.9	0.67	4.26E-05
1.15	Opx	Sp Harzburgite	XML11	0.11766	1.38E-17	1.42E-12	2.25E-14	6.73E-17	2.28E-15	4.20E-07	5.08E-09	1.37E-11	1.13E-14	1.03E-11	62.8	0.14	3.37E-06
1.15	Cpx	Sp Harzburgite	XML11	0.05385	3.62E-17	3.55E-12	2.73E-14	7.92E-17	2.79E-15	3.33E-07	4.70E-09	1.76E-11	2.18E-14	1.11E-11	129.9	0.32	1.07E-05
1.2	Ol	Sp Lherzolite	XML6	0.52471	4.80E-17	4.32E-12	7.10E-15	2.19E-17	7.06E-16	6.73E-09	8.79E-11	6.89E-12	6.24E-15	5.04E-12	608.5	0.86	6.42E-04
1.2	Opx	Sp Lherzolite	XML6	0.10331	4.72E-17	4.39E-12	1.06E-14	3.30E-17	1.05E-15	1.37E-07	4.42E-09	2.25E-11	4.98E-15	2.10E-11	415.8	0.21	3.21E-05
1.2	Cpx	Sp Lherzolite	XML6	0.04105	8.66E-17	8.21E-12	1.45E-14	4.49E-17	1.42E-15	8.12E-07	1.18E-08	1.33E-10	3.35E-14	1.24E-10	565.4	0.07	1.01E-05
1.22	Ol	Sp Lherzolite	XML8	0.50752	7.62E-18	7.66E-13	9.87E-16	3.10E-18	9.38E-17	5.31E-10	4.89E-11	1.31E-12	8.91E-16	1.04E-12	776.1	0.73	1.44E-03
1.22	Opx	Sp Lherzolite	XML8	0.31254	3.26E-17	3.29E-12	6.44E-15	1.91E-17	6.48E-16	5.59E-08	1.95E-09	3.91E-12	3.74E-15	2.81E-12	511.8	1.17	5.89E-05
1.23	Ol	Sp Harzburgite	XML5	0.50783	2.58E-17	2.49E-12	1.24E-14	3.74E-17	1.24E-15	4.38E-08	6.77E-10	4.92E-11	9.48E-15	4.64E-11	200.7	0.05	5.69E-05
1.23	Opx	Sp Harzburgite	XML5	0.10976	1.80E-17	1.71E-12	2.59E-14	7.87E-17	2.61E-15	4.13E-07	5.74E-09	3.55E-11	1.13E-14	3.22E-11	66.0	0.05	4.14E-06
1.23	Cpx	Sp Harzburgite	XML5	0.058	3.64E-18	4.93E-13	8.37E-14	2.50E-16	8.53E-15	5.19E-07	4.57E-09	4.47E-11	5.41E-14	2.87E-11	5.9	0.02	9.50E-07
1.3	Ol	Sp Harzburgite	-	0.52935	3.76E-17	3.57E-12	6.05E-15	1.82E-17	6.03E-16	5.75E-09	n.a	6.39E-12	6.12E-15	4.58E-12	589.8	0.78	6.20E-04
1.3	Opx	Sp Harzburgite	-	0.10888	7.71E-17	7.27E-12	3.62E-14	1.07E-16	3.63E-15	6.92E-07	8.23E-09	2.83E-11	1.43E-14	2.40E-11	200.7	0.30	1.05E-05
1.3	Cpx	Sp Harzburgite	-	0.05363	2.26E-16	2.13E-11	3.37E-14	1.06E-16	3.33E-15	2.17E-06	4.02E-08	5.81E-11	3.26E-14	4.85E-11	631.8	0.44	9.78E-06

664

665

666

667

668

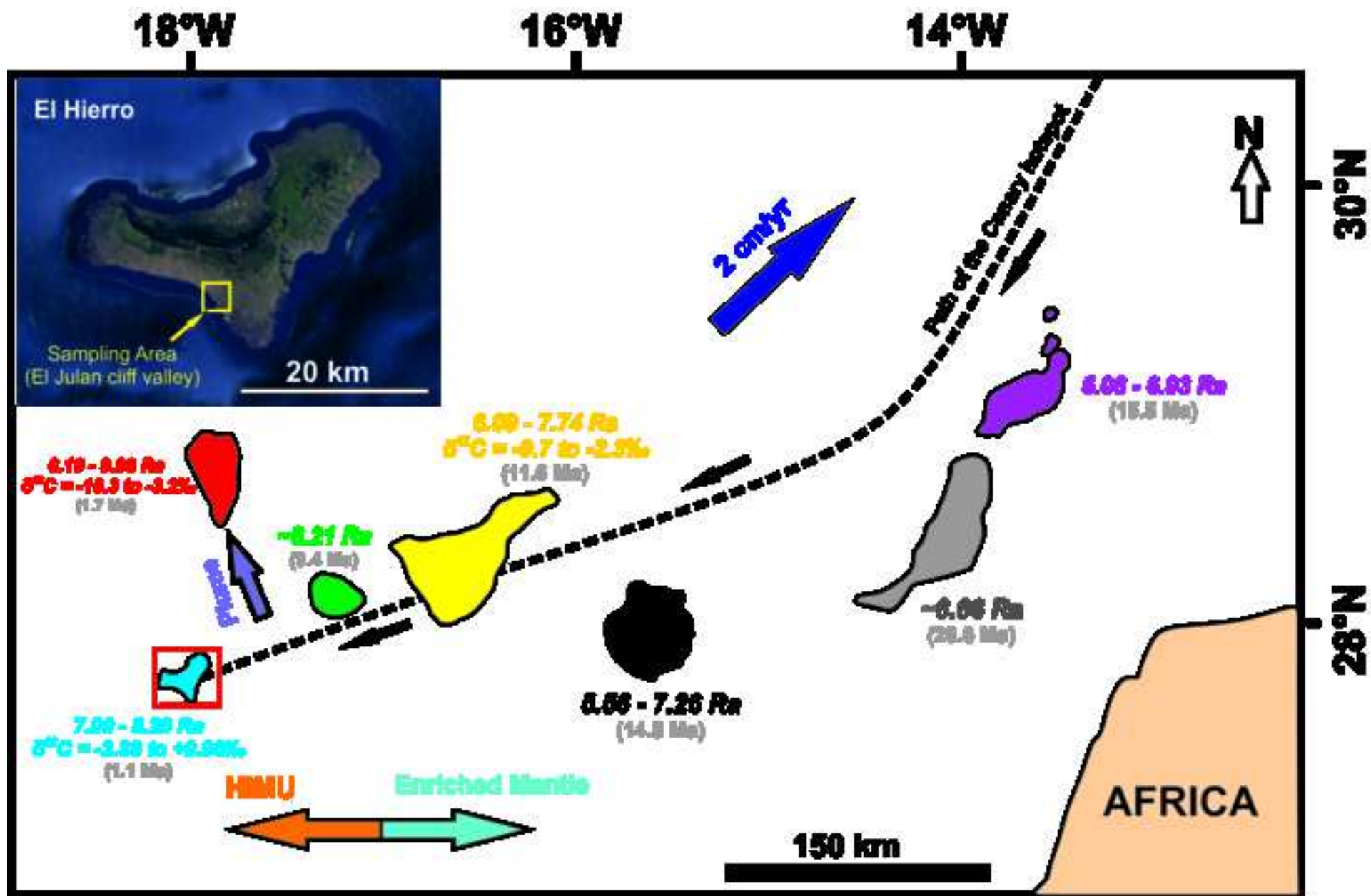
Table 1. Continued.

Sample	Mineral	R/Ra	Rc/Ra <sup>E</sup>	Error (+/-)	<sup>40</sup> Ar/ <sup>36</sup> Ar	Error (+/-)	<sup>38</sup> Ar/ <sup>36</sup> Ar	Error (+/-)	<sup>20</sup> Ne/ <sup>22</sup> Ne	Error (+/-)	<sup>21</sup> Ne/ <sup>22</sup> Ne	Error (+/-)	CO <sub>2</sub> / <sup>3</sup> He	<sup>3</sup> He/ <sup>36</sup> Ar	CO <sub>2</sub> <sup>B</sup>	CO <sub>2</sub> / <sup>3</sup> He <sup>B</sup>	δ <sup>13</sup> C (‰)
1.1	Ol	7.20	7.21	0.16	4141.0	0.0	0.1880	0.0007	10.11	0.07	0.0304	0.00106	2.09E+09	5.47E-03	n.a	n.a	n.a
1.1	Opx	4.41	4.43	0.25	2734.4	97.7	0.1880	0.0007	10.04	0.16	0.0319	0.00249	6.64E+09	9.33E-04	n.a	n.a	n.a
1.1	Cpx	5.76	5.85	0.57	5328.4	76.0	0.1946	0.0008	9.87	0.14	0.0302	0.00161	5.98E+10	1.09E-04	n.a	n.a	n.a
1.15	Ol	7.44	7.45	0.15	2620.4	0.0	0.1831	0.0007	9.99	0.04	0.0296	0.00081	2.26E+09	1.60E-02	5.53E-08	1.48E+09	0.96
1.15	Opx	6.98	7.01	0.21	1210.0	11.8	0.1864	0.0007	9.94	0.06	0.0297	0.00120	3.04E+10	1.22E-03	2.75E-07	1.99E+10	-1.23
1.15	Cpx	7.33	7.34	0.21	805.0	6.4	0.1908	0.0007	9.84	0.11	0.0286	0.00121	9.19E+09	1.66E-03	n.a	n.a	n.a
1.2	Ol	7.99	7.99	0.15	1103.1	0.0	0.1848	0.0007	10.12	0.05	0.0312	0.00095	1.40E+08	7.69E-03	n.a	n.a	n.a
1.2	Opx	7.72	7.73	0.18	4516.6	76.2	0.2005	0.0008	10.40	0.13	0.0325	0.00230	2.90E+09	9.48E-03	2.67E-07	5.65E+09	-1.43
1.2	Cpx	7.59	7.59	0.20	3979.1	39.8	0.1654	0.0005	10.43	0.24	0.0323	0.00245	9.38E+09	2.58E-03	n.a	n.a	n.a
1.22	Ol	7.16	7.16	0.17	1465.4	0.0	0.1764	0.0006	10.49	0.24	0.0330	0.00390	6.96E+07	8.55E-03	n.a	n.a	n.a
1.22	Opx	7.11	7.11	0.16	1044.6	12.7	0.1861	0.0007	9.98	0.09	0.0296	0.00143	1.72E+09	8.70E-03	n.a	n.a	n.a
1.23	Ol	7.46	7.47	0.15	5187.2	0.0	0.2002	0.0008	10.09	0.04	0.0304	0.00081	1.69E+09	2.73E-03	1.28E-08	4.95E+08	-0.19
1.23	Opx	7.52	7.55	0.19	3137.1	37.6	0.1957	0.0008	10.01	0.07	0.0304	0.00136	2.30E+10	1.59E-03	3.64E-07	2.03E+10	-2.38
1.23	Cpx	5.07	5.32	0.40	826.7	2.9	0.1877	0.0007	9.84	0.06	0.0295	0.00076	1.42E+11	6.74E-05	n.a	n.a	n.a
1.3	Ol	7.58	7.59	0.15	1043.7	0.0	0.1846	0.0007	10.05	0.07	0.0303	0.00118	1.53E+08	6.15E-03	n.a	n.a	n.a
1.3	Opx	7.62	7.63	0.17	1975.5	12.8	0.1887	0.0007	10.04	0.06	0.0297	0.00109	8.98E+09	5.39E-03	5.09E-07	6.60E+09	-1.94
1.3	Cpx	7.65	7.66	0.16	1780.7	10.5	0.1888	0.0007	10.18	0.09	0.0321	0.00161	9.60E+09	6.94E-03	9.47E-07	4.19E+09	-1.94

C. N<sub>2</sub>\*: N<sub>2</sub> values corrected for atmospheric contamination during the simultaneous extraction of CO<sub>2</sub> and noble gases.

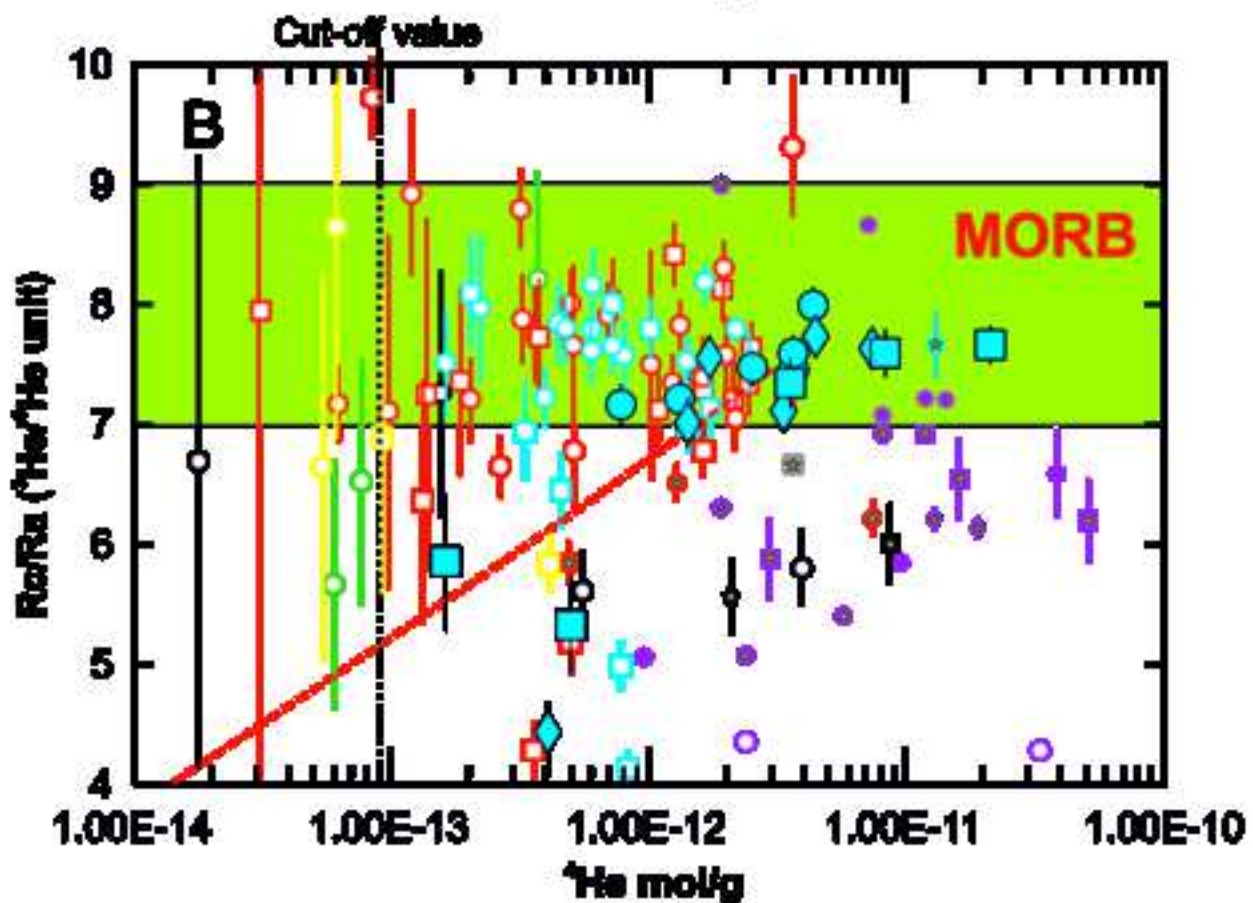
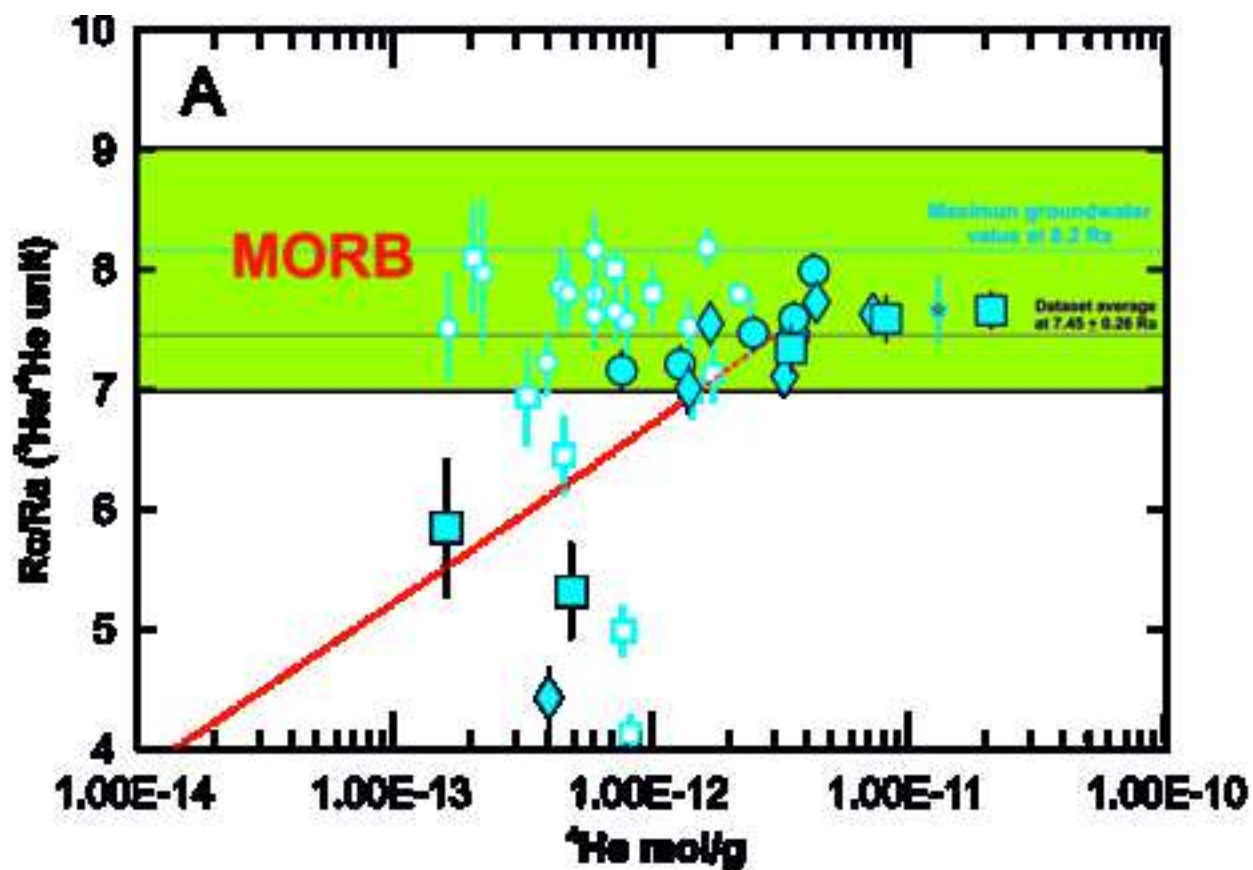
D. <sup>40</sup>Ar\*: <sup>40</sup>Ar values corrected for atmospheric contamination.  $^{40}\text{Ar}^* = ^{40}\text{Ar}_{\text{sample}} - (^{36}\text{Ar}_{\text{sample}} \cdot (^{40}\text{Ar}/^{36}\text{Ar})_{\text{air}})$ . Where  $^{40}\text{Ar}/^{36}\text{Ar}_{\text{air}} = 295.5$

E. Rc/Ra: R/Ra ratio corrected for atmospheric contamination.  $\text{Rc/Ra} = ((\text{R/Ra})_{\text{sample}} \cdot (^{4}\text{He}/^{20}\text{Ne})_{\text{sample}} - (^{4}\text{He}/^{20}\text{Ne})_{\text{air}}) / ((^{4}\text{He}/^{20}\text{Ne})_{\text{sample}} - (^{4}\text{He}/^{20}\text{Ne})_{\text{air}})$ . Where  $^{4}\text{He}/^{20}\text{Ne}_{\text{air}} = 0.318$

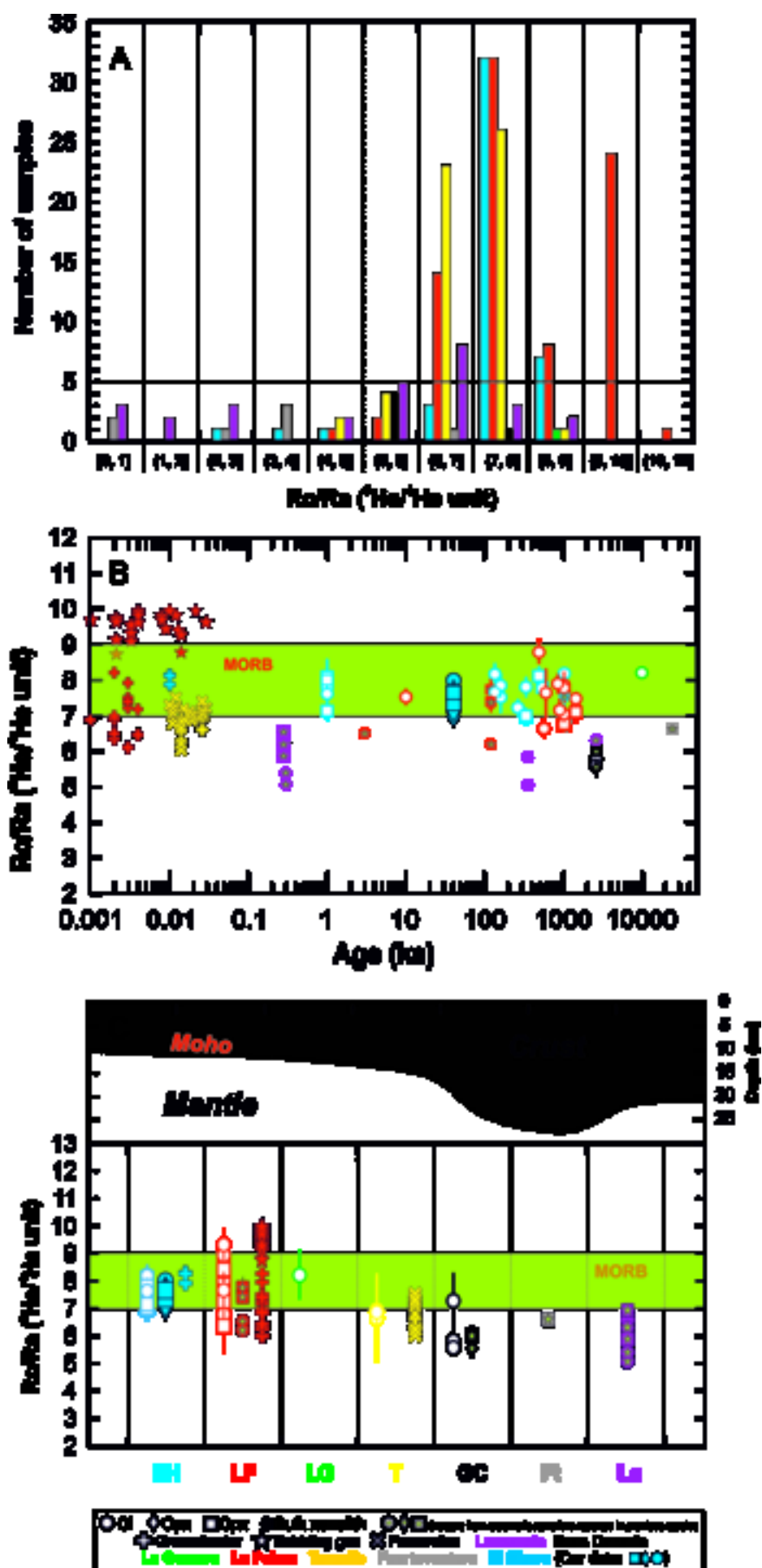


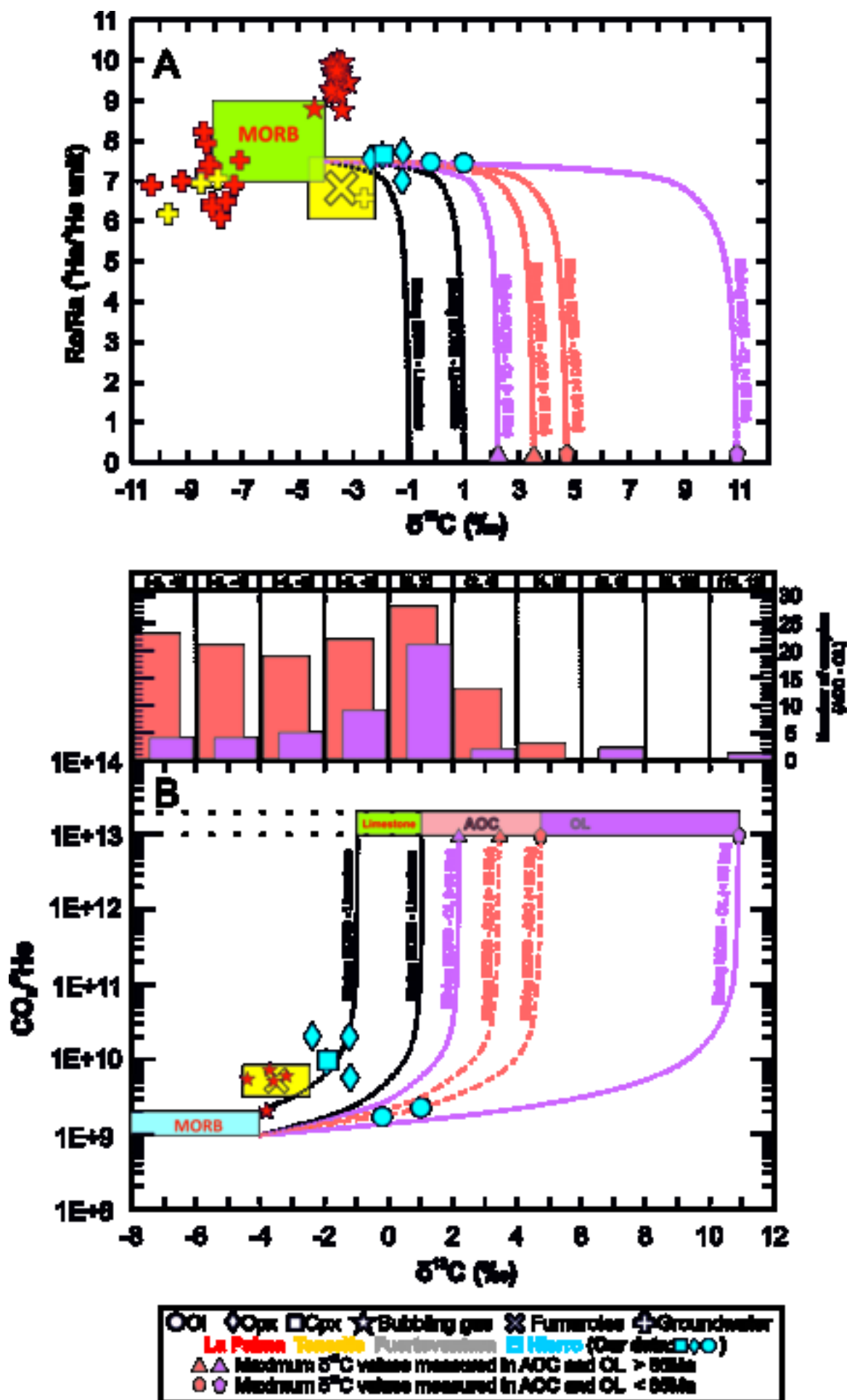
■ El Hierro 
 ■ La Palma 
 ■ La Gomera 
 ■ Tenerife 
 ■ Gran Canaria 
 ■ Fuerteventura 
 ■ Lanzarote













Click here to access/download

**Supplementary material/Appendix (Files for online  
publication only)**  
Table S1.xlsx



Click here to access/download

**Supplementary material/Appendix (Files for online  
publication only)**  
Table S2.xlsx



Click here to access/download

**Supplementary material/Appendix (Files for online  
publication only)**

Supplementary material\_Sandoval-Velasquez et al.docx

**Declaration of interests**

The authors declare that they have no known competing financial interests or personal relationships that could have appeared to influence the work reported in this paper.

The authors declare the following financial interests/personal relationships which may be considered as potential competing interests: